Monthly Notices
of the
ROYAL ASTRONOMICAL SOCIETY

MNRAS **477,** 3257–3272 (2018)
Advance Access publication 2018 March 3

doi:10.1093/mnras/sty572

On the possibility that ultra-light boson haloes host and form supermassive black holes

Ana A. Avilez,[1]★ Tula Bernal,[2]★ Luis E. Padilla[1]★ and Tonatiuh Matos[1]†

[1]*Departamento de Física, Centro de Investigación y de Estudios Avanzados del IPN, AP 14-740, Ciudad de México 07000, México*
[2]*Universidad Autónoma Chapingo, km. 38.5 Carretera México-Texcoco, 56230 Texcoco, Estado de México, México*

Accepted 2018 February 23. Received 2018 January 26; in original form 2017 April 22

ABSTRACT

Several observations suggest the existence of supermassive black holes (SMBH) at the centres of galaxies. However, the mechanism under which these objects form remains non-completely understood. In this work, we review an alternative mechanism of formation of galactic SMBHs from the collapse of a fraction of a dark matter (DM) halo made of an ultra-light scalar field (SF) whose critical mass of collapse is $\sim 10^{13}\,M_{\odot}$. Once the BH is formed, a long-living quasi-resonant SF configuration survives and plays the role of a central fraction of the galactic DM halo. In this work, we construct a model with an ultra-light SF configuration laying in a Schwarzschild space–time to describe the centre of the DM halo hosting an SMBH in equilibrium, in the limit where self-gravitating effects can be neglected. We compute the induced stellar velocity dispersion in order to investigate the influence of the BH on to the velocity field of visible matter at the central galactic regions. We fit the empirical correlation between stellar velocity dispersions and masses of SMBHs considering two instances: the idealized case of DM-dominated (DMD) systems, where the gravitational influence of baryons is neglected, and cases of real luminous galaxies (LGAL). In the DMD case, we found it is possible to reproduce the observed stellar velocity dispersions at the effective radius of systems hosting SMBHs of at most $10^{8}\,M_{\odot}$. In the LGAL case, we found that the baryons are crucial to reproduce the observed velocity dispersion.

Key words: gravitation – galaxies: haloes – quasars: supermassive black holes – dark matter.

1 INTRODUCTION

A host of observations indicate the existence of supermassive black holes (SMBH) placed at the centre of the most luminous galaxies. SMBHs are enormous in comparison to stellar black holes, their masses may run between 10^{6} and $10^{10}\,M_{\odot}$ (Lynden-Bell 1969; Cappellari 2011; McConnell et al. 2011). An open problem regarding SMBHs based on observations is why their masses M at the centres of galaxies correlate with various global properties of the stellar components. The most important relationships occur between M and the bulge mass, and a tighter correlation between M and the stellar velocity dispersion of the host galaxy bulge, first reported in Merritt & Ferrarese (2001) and Gebhardt et al. (2000), suggesting that the formation and evolution of SMBHs and the bulge of the parent galaxy may be closely related.

Although many research groups are trying to understand how these objects were formed, their origin is still mysterious due to their huge mass and the large redshift at which they have been observed (Netzer 2003; Genzel 2017). Between the most popular proposals of formation mechanisms of SMBHs is that, likewise stellar BHs which result from the collapse of massive stars, SMBHs are produced by the collapse of massive clouds of gas during the early stages of formation of a galaxy (Silk & Rees 1998). Another common idea is that a stellar BH becomes supermassive by Eddington-rate accretion of large amounts of baryonic material and cold dark matter (CDM) during their quasar phase (Yu & Tremaine 2002; Larkin & McLaughlin 2016). Another suggestion is that clusters of stellar BHs are formed and eventually merge into an SMBH (Menou, Haiman & Narayanan 2001). However, so far under this standard scenario, there is not a fully satisfactory explanation for the formation and evolution of such SMBHs at large redshifts, even taking into account effects coming from baryonic matter physics. For that reason, in this work we consider a novel alternative of formation of SMBHs starting from the hypothesis that galactic haloes are made of ultra-light bosons, all laying in the ground state and therefore making up a Bose–Einstein condensate (BEC) which can be described by a configuration made of classical scalar field (SF) solutions. At certain moment in the cosmic history, when the configuration reaches a critical mass, it starts to collapse into a BH. Based in results from Escorihuela-Tomas et al. (2017) and

★ E-mail: aavilez@fis.cinvestav.mx (AAA); ac13341@chapingo.mx (TB); epadilla@fis.cinvestav.mx (LEP)
† Part of the Instituto Avanzado de Cosmología (IAC) collaboration (http://www.iac.edu.mx).

Herdeiro & Radu (2014), we argue that once after the BH is formed, a quasi-resonant solution of SF may constitute the centre of the dark matter (DM) halo, which in despite of being a decaying solution, it survives a time-length as large as the age of the Universe, as shown in Barranco et al. (2011, 2012) and Guzman & Lora-Clavijo (2012). Recent detections of SMBHs at the centres of dense dwarf galaxies in the Virgo cluster strongly support this idea. The fact that the masses of these 'mammoth' SMBHs are of the same order of magnitude than their host galaxies suggests that these galaxies were giant galaxies at early times (Drinkwater et al. 2000; King 2016; Ahn et al. 2017).

It is worth to make a parenthesis here in order to highlight that this ultra-light boson DM candidate is a strong and well studied alternative to the CDM paradigm. It is usually known as scalar field dark matter (SFDM), which proposes the DM is composed by spin-0, self-gravitating ultra-light bosons described by the Einstein–Klein–Gordon (EKG) system. The boson mass runs in the range $m \sim 10^{-23}$–$10^{-21}\,\mathrm{eV\,c^{-2}}$, and it might be self-interacting. At very large scales the predictions from this model are the same than those of the ΛCDM model (Rodríguez-Montoya et al. 2010; Suárez & Matos 2011; Magaña et al. 2012), where Λ is the cosmological constant, since it reproduces, within 1σ of confidence, the cosmic microwave background and the mass power spectrum of matter at large scales, where the linear regime of the cosmological perturbation theory holds (see also Hlozek et al. 2015; Schive et al. 2016). It has been shown that these systems made of ultra-light bosons form BECs making up the galactic haloes (Matos & Arturo Ureña-López 2001). This alternative naturally solves the CDM problems at the galactic scales: the ultra-light masses of the SF particles provides a solution to the 'core-cusp' problem (see e.g. Moore et al. 1999; de Blok et al. 2001; McGaugh et al. 2007; de Blok 2010; Amorisco & Evans 2012; Peñarrubia et al. 2012; Walker 2013; Del Popolo & Pace 2016, among others), it prevents the overabundance of small haloes and the 'too-big-to-fail' problems (see e.g. Klypin et al. 1999; Kroupa et al. 2010; Boylan-Kolchin, Bullock & Kaplinghat 2011; Pawlowski, Pflamm-Altenburg & Kroupa 2012; Peñarrubia et al. 2012; Sawala et al. 2016, among others), and it also predicts the early formation of big galaxies at very high redshifts (Caputi et al. 2015). The idea of the SFs as the DM of the Universe was first suggested in Baldeschi, Gelmini & Ruffini (1983); since then the idea was rediscovered several times dubbed with different names (see e.g. Membrado, Pacheco & Sañudo 1989; Press, Ryden & Spergel 1990; Ji & Sin 1994; Sin 1994; Lee & Koh 1996; Goodman 2000; Matos & Ureña-López 2000; Peebles 2000; Sahni & Wang 2000; Arbey, Lesgourgues & Salati 2001; Matos & Arturo Ureña-López 2001; Wetterich 2001; Woo & Chiueh 2009; Lundgren et al. 2010; Calabrese & Spergel 2016; Schwabe, Niemeyer & Engels 2016; Hui et al. 2017; Mocz et al. 2017, among others), for example: SFDM (Matos & Guzman 2000), fuzzy DM (Hu, Barkana & Gruzinov 2000), wave DM (Bray 2010; Schive et al. 2014), BEC DM (Böhmer & Harko 2007), or ultra-light axion DM (Marsh & Ferreira 2010). However, the first systematic study of this idea was started in Guzmán & Matos (1998) and Guzman, Matos & Villegas (1999). The cosmological regime of this model was first studied in Matos, Guzman & Urena-Lopez (2000) and Matos & Arturo Ureña-López (2001). In such work observational counts of nearby satellite galaxies were used to estimate the mass of the ultra-light bosons to be $m \sim 10^{-22}\,\mathrm{eV\,c^{-2}}$, since the model presents a cut-off in the power spectrum which suppresses the small-scale structure formation for halo masses $M < 10^{8}\,\mathrm{M_{\odot}}$ (see also Schive et al. 2014; Ureña-López & Gonzalez-Morales 2016; Hidalgo et al. 2017). The mass of the ultra-light boson has been constrained from several cosmological and astrophysical observations, for example, from the galaxy UV-luminosity function and reionization data (Hlozek et al. 2015), from the high-redshift luminosity function of galaxies (Schive et al. 2016), from Lyman α observations (Sarkar et al. 2016; Armengaud et al. 2017; Iršič et al. 2017), taking into account a self-interaction into the SF potential (Li, Rindler-Daller & Shapiro 2014). However, there is not an agreement on the correct mass of the ultra-light boson. In this work we use the value $m \sim 10^{-22}\,\mathrm{eV\,c^{-2}}$. At galactic scales, SFDM haloes are described as gravitationally bound solutions of the Schrodinger–Poisson and Gross–Pitaevskii–Poisson systems (Guzmán & Ureña-López 2004, 2006), which are the weak-gravity version of the EKG equations in the Newtonian limit, neglecting or including self-interactions. In multiple astrophysical applications the hydrodynamical formulation of Einstein-Klein-Gordon system has been developed in flat and curved spaces (Matos et al. 2016). It has been shown in a series of papers that such an approach suffices to reproduce the stellar rotation curves of many galaxies (Guzmán & Matos (1998); Bernal, Matos & Núñez 2008; Harko 2011; Robles & Matos 2012, 2013b; Martinez-Medina & Matos 2014; Bernal et al. 2017a), the velocity dispersions observed in dwarf spheroidal galaxies (Marsh & Pop 2015; Martinez-Medina, Robles & Matos 2015; Chen, Schive & Chiueh 2017; González-Morales et al. 2017) and the dynamical masses inferred from X-ray galaxy cluster observations (Bernal, Robles & Matos 2017b), among others.

Since a key hypothesis of this work is that BHs may form from the collapse of SF configurations, let us now briefly make a historical review of the study of stability conditions and the process of collapse of these objects. The problem of collapse of SF configurations has been extensively studied during the last few decades in many contexts. First, by analysing different regimes of stability (or instability) of SF solutions, different groups have arrived to remarkable insights about spherical self-gravitating BECs (Seidel & Suen 1990, 1991, 1994; Alcubierre et al. 2002a,b; Barranco et al. 2011, 2012; Cruz-Osorio, Guzmán & Lora-Clavijo 2011; Chavanis 2016; Sanchis-Gual et al. 2017). The typical systems considered for these studies have been boson stars and therefore they are limited to explain the formation of stellar BHs. In this work, we aim to set some basis to extend those approaches for larger systems, like SFDM haloes of galaxies where SMBHs are typically observed. The formation mechanism of SMBHs proposed in all those works, provides a natural way to explain the huge masses of even the biggest SMBH observed so far (up to $10^{12}\,\mathrm{M_{\odot}}$). Besides, it has been shown in Barranco et al. (2011, 2012), Herdeiro & Radu (2014), and Sanchis-Gual et al. (2017) that after the collapse a remaining solution of SF survives for sufficiently large time so they can be used to model the central part of DM haloes being influenced by the BH. However, provided that in all the numerical simulations enlisted above, spherical symmetry (or axial symmetry at most) is assumed and that they use a quite limited set of initial conditions, the structure and mass of the complete remaining halo is far from being realistically modelled by those approaches, as we explain later. A first important result from some pioneer numerical simulations of Seidel & Suen (1990, 1994) and Alcubierre et al. (2002b) is that SF configurations made of bosons with ultra-light mass can collapse as long as their masses lay around ($\sim 10^{12}\,\mathrm{M_{\odot}}$), that is, close to the mass of a Milky Way-like halo, ending up into a BH at the centre of the system which is slightly less massive than the seed halo. Secondly, in despite that the no-hair theorems forbid static solutions (hair) to exist around the BHs (Bekenstein 1995; Gürlebeck 2015), nothing prevents the existence of decaying solutions around them with lifetimes compared to cosmic times (Barranco et al. 2011, 2012; Sanchis-Gual

et al. 2017) and they can clearly play the role of a fraction of the DM galactic halo (Myung, Kim & Park 2008). Moreover, numerical simulations from Herdeiro & Radu (2014) and Escorihuela-Tomas et al. (2017), assuming spherical and axial symmetries, show that a large fraction of the SF collapses into a BH and a small fraction of the SF remains in the surroundings.

Although so far the possibility of formation of SMBHs in this scenario is widely studied, further studies are needed in order to construct a realistic model to describe a galactic system. Particularly, it is imperative to carry out simulations of the collapse of SF configurations relaxing the spherical symmetry assumption and taking into account other highly non-linear phenomena. Nevertheless, intuitively we may have some insights about some additional effects in a 3D system. For example, let us think in a primordial perturbation of SFDM in the unstable collapsing branch defined in Seidel & Suen (1991), that is, with a mass laying around $10^{12}\,M_{\odot}$ and having a central value larger than the critical one. According to the results from numerical simulations in spherical symmetry performed so far, the most part of an initial perturbation (which has a very specific shape by the way) would collapse into a BH (Escorihuela-Tomas et al. 2017). In contrast, for a 3D system, along with further effects, diverse initial configurations are allowed and consequently the conditions and mechanisms of collapse would be different. Particularly, for rotating initial configurations, it is possible that, because of the centripetal force, at some critical value, a fraction of the SF perturbation at the outer regions tears apart from a central one and therefore the SF at the centre is able to collapse while the external fraction could avoid the gravitational pull towards the centre. Although some steps have been already done in studying SF hair in static rotating systems considering Kerr BHs (Herdeiro & Radu 2014), the whole non-linear relativistic process and more general stability conditions, must be studied by means of numerical simulations (at least axial symmetric) in the future.

Besides the cumbersome and highly non-linear set of coupled equations describing the collapse of an SF configuration, another complication of working with galactic systems is that the physics of the BH happens at a spatial scale of $\sim 10^{-6}$ pc, while that of the galaxy does at 10–30 kpc. Dealing with such a huge gap of scales requires tremendous numerical resources. Nevertheless, through gathering together the previous numerical work regarding systems at stellar scales and physical arguments, we can construct idealized approaches in order to study, at some extent, the viability of this scenario. Based in the results mentioned above, this work stands over two main hypotheses given by (i) the formation of SMBHs is due to the collapse of a fraction of the central region of an SFDM halo and (ii) in the final galactic systems the central part of the SFDM halo corresponds to a quasi-resonant solution of the SF decaying very slowly into the SMBH, such that it survives at least a cosmic time.

In this work, we aim starting to address this problem in a semi-analytical way, starting from the simplest scenario: we assume that the galactic SFDM halo lives in a Schwarzschild space–time. This is valid if we consider the quasi-static limit, in this case we are assuming that the BH has been already formed and that the remaining SFDM halo corresponds to a long-living spherical quasi-resonant solution. It is worth to mention that in this approach the back-reaction either of the scalar and visible matter on to the metric is neglected. Since the space–time is assumed to have Schwarzschild geometry, the black hole is the only one that has a gravitational contribution at the level of the field equations. None the less, these simplifications are worth since we derive an analytical approximation for the density profile of DM in the faraway neighbourhood of a black hole instead of solving the highly non-linear fully relativistic EKG system.

We solve analytically the Klein–Gordon (KG) equation in a Schwarzschild space–time with spherical symmetry assuming the observer is placed far away from the BH and for scales lower than the characteristic length of the SFDM configuration, where the self-gravity effects of the scalar and BH can be neglected (see Appendix). We have found that our analytical solution is indistinguishable from SFDM profiles at the outer regions, that is, for scales larger than the characteristic length of the SF configuration, where the rotation curves are usually measured. The SFDM density profile is only modified close to the centre, where SMBHs are detected from observations of the kinematics of visible matter. We refer to these kind of solutions as Schwarzschild-scalar field dark matter (SSFDM).

Now, a surprising fact involving SMBHs and their host galaxies is the correlation between the mass of the SMBH and the velocity dispersion of stars and gas at the galactic centres (Gebhardt et al. 2000; Merritt & Ferrarese 2001; Ferrarese & Ford 2005; McConnell & Ma 2013). Usually, this connection is attributed to accretion winds feedback of the BH into the baryonic matter laying in the bulge (Larkin & McLaughlin 2016). However, although the accretion winds could highly affect the stellar kinematics up to some point, we argue that given the difference of scales at which both phenomena occur, the correlation between both thresholds still remains as a mystery and may be triggered by a different mechanism. Moreover, in the galaxies sample used to infer this correlation, there are galaxies out of their accretion phase; therefore, the former scenario fails to explain why they still fulfil the correlation. Additionally, SMBHs are not observed directly, in turn their properties (mass and angular momentum) are inferred from features of the velocity field of stars in the galactic bulge, particularly the velocity dispersion of stars (McConnell & Ma 2013). Therefore, any framework designed to describe the joint dynamics of an SMBH and its host galaxy should be able to fit the observed stellar velocity dispersions.

In this work, we compute theoretical predictions of the mean velocity dispersions corresponding to each solution for a fixed mass of the BH, for different values of the characteristic length of the profile. We achieve this by solving the isotropic Jeans equation and modelling the density and mass distributions using the phenomenological Plummer profile (Plummer 1911) which is suitable to describe density distributions of spherical stellar systems like bulges, dwarf and elliptical galaxies (Walker et al. 2009; Ahn et al. 2017).

In order to fully construct an SFDM profile in a space–time surrounding an SMBH which is compatible with observations, we determine values of the free parameters central density and characteristic length of the SF configuration, using theoretical and observational constraints. First, by imposing boundary conditions on the classical solutions of the KG equation, we derive an upper bound for the characteristic length of the SF configuration, as performed in Barranco et al. (2011). Secondly, we reduce the space of parameters of our solutions, by establishing a relation between the central density of the SFDM profile and its characteristic length by considering the universality of the maximum acceleration of DM particles reported in Ureña-López, Robles & Matos (2017). This result was recently derived from the mass discrepancy–acceleration relation (MDAR) coming from observations of a large set of galaxies (McGaugh, Lelli & Schombert 2016; Lelli et al. 2017). A complementary result of the present work is a modification on the constraint over the central surface density found in Ureña-López et al. (2017), but introducing the effect of a BH. We carry out their analysis for the special sort of galaxies hosting SMBHs, and found a maximal

relation between the DM central surface density and the mass of the BH, which corresponds to an increasing function, a result consistent with previous results (Barranco et al. 2011, 2012; Lee, Lee & Kim 2015).

Finally, for each value in the considered range of masses of the BH, we fix value of the characteristic length of the SFDM profile such that the theoretical stellar velocity dispersion fits the corresponding value given by the M–σ^* correlation reported in McConnell & Ma (2013). We carry out such procedure in two different cases: (1) DM-dominated (DMD) systems: in this idealized case the gravitational potential of DM dominates within the Jeans equation. Although this scenario is still hypothetical, it is potentially interesting observationally since it could be useful for studying ultra-compact dwarf (UCD) galaxies in the future when further information about these sort of systems becomes available. (2) Real luminous galaxies (LGAL): we solved the Jeans equation for a catalogue of six luminous galaxies housing SMBHs in their centres. In contrast to DMD, in this case, the profiles for the visible matter are already known. Additionally, the gravitational contributions of dark and visible matter are considered within the Jeans equation. From the results from the fits in each case we can conclude: in the DMD case, we found that it is possible to predict the observed stellar velocity dispersion for galaxies hosting SMBH with masses smaller than $10^8\,\mathrm{M}_\odot$. In the LGAL, by considering all the galactic matter contributions, it is possible to reproduce σ^* for all galaxies in our catalogue.

Now, we would like to point out that, in despite of the simplicity of this model, it is worth to keep studying and improving it, since it has been helpful to reproduce the observed values of velocity dispersion of stars in the LGAL case (taking into account the importance of baryons) and it gives us an idea of the power of predictability of the DMD case for modelling hypothetical low-brightness galaxies with BHs with masses up to $10^8\,\mathrm{M}_\odot$. Furthermore, recently an international team of astronomers used an Earth-sized telescope formed as a series of telescopes placed across the globe, known as the Event Horizon Telescope (EHT), to obtain for the very first time a direct image of Sagittarius A (the SMBH hosted at the centre of the Milky Way) (Eve 2015; Ricarte & Dexter 2015). Observations of the deep-inner galactic region are very likely to be improved in short time and this would bring up a new source of evidence of the properties of the SMBH and its influence on stars laying in the galactic bulge. Particularly, it might be possible to obtain a direct measurement of the mass and angular momentum of these objects. In addition, from observations of the stellar evolution across this region, wealthy information of the DM configurations would be inferred, which would be useful to discriminate between different DM models. Either to test our hypothesis about SMBH formation and to compare different DM models in the deep-inner galactic regions using these and upcoming direct observations of SMBHs in a short future is a compelling goal that we are after.

The paper is organized as follows: In Section 2, we make a brief review on the research work about the collapse of an SF configuration into a BH. In Section 3, we state our hypotheses. In Section 4, we present our model and analyse some conditions over the spectrum of solutions; we derive the general KG equation in a Schwarzschild space–time, consider the limit for radii far away from the horizon of the SMBH and solve it analytically. In Section 5, we treat the same equation perturbatively, such that it turns into an equation for a forced oscillator, helping us to understand the perturbative effect of the BH over SFDM solutions in a more intuitive way. In Section 6, we compute and study SFDM density and mass profiles from our exact solution. In Section 7, we reduce our space of parameters by imposing a relation between the central density of the profile and the characteristic length. We extend the constraint on the central surface density from Ureña-López et al. (2017) for galaxies housing SMBHs, for the SSFDM model proposed here. In Section 8, we constrain the characteristic length of the profile by fitting measurements of the mean velocity dispersion of a number of real elliptical galaxies and bulges hosting SMBHs. Finally, in Section 9, we present our discussion and conclusions.

2 BRIEF HISTORICAL REVIEW OF THE PROBLEM: COLLAPSE OF SFDM CONFIGURATIONS

The pioneering studies of equilibrium configurations of self-gravitating bosons in the ground state (Ruffini & Bonazzola 1969) show that the maximum mass of an SF configuration depends on the mass of the boson. This critical mass is understood as follows: for a system of N self-gravitating bosons such that $N > N_{\mathrm{crit}}$, a critical number of bosons, the gravitational collapse actually occurs. In the non-self-interacting case they found that the critical mass of collapse is given by

$$M_{\mathrm{crit}} \sim \frac{m_{\mathrm{Pl}}^2}{m}, \tag{1}$$

where m_{Pl} is the Planck mass and m is the mass of the SF. At this critical value, the binding energy per particle becomes comparable to the rest energy. For a system with a number of particles $N > N_{\mathrm{crit}}$, there exists non-equilibrium configurations of self-gravitating bosons in their ground state. For the ultra-light bosons, we study here with masses between $m \sim 10^{-23}$ and $10^{-22}\,\mathrm{eV\,c^{-2}}$, the critical mass of collapse lays between $M_{\mathrm{crit}} \sim 2.8 \times 10^{11}$ and $2.8 \times 10^{12}\,\mathrm{M}_\odot$. Later, by means of numerical simulations assuming spherical symmetry, Seidel & Suen (1991, 1994) figure out a more precise relation for the critical mass of collapse of a system of bosonic particles given by

$$M_{\mathrm{crit}} \sim 0.6\frac{m_{\mathrm{Pl}}^2}{m}. \tag{2}$$

Later on, numerical simulations from Alcubierre et al. (2002a,b) revealed that the critical mass of collapse in order to form stable solutions from an initial SF perturbation with a cosh -like potential is given by $M_{\mathrm{crit}} \sim 10^{13}\,\mathrm{M}_\odot$ for a boson mass $m = 1.1 \times 10^{-23}\,\mathrm{eV\,c^{-2}}$. For the boson mass $m \sim 10^{-22}\,\mathrm{eV\,c^{-2}}$, the critical mass was found to be $M_{\mathrm{crit}} \sim 10^{12}\,\mathrm{M}_\odot$, which corresponds to the typical mass of a Milky Way-like halo.

For SFDM configurations including excited states of an SF with a given mass (Seidel & Suen 1990; Hawley & Choptuik 2003; Ureña-López 2009; Bernal et al. 2010; Ureña-López & Bernal 2010), it was found that the resulting configurations can have larger masses since they reach new equilibrium configurations through mass-loss (gravitational cooling).

In the case of a self-interacting SF ϕ with the simplest ϕ^4-potential given by

$$V(|\phi|^2) = m^2\phi^2 + \frac{\lambda}{2}|\phi|^4, \tag{3}$$

the critical mass of collapse reads (Colpi, Shapiro & Wasserman 1986)

$$M_{\mathrm{crit}} \sim 0.22\sqrt{\Lambda}\frac{m_{\mathrm{Pl}}}{m^2}, \tag{4}$$

where $\Lambda \equiv \lambda/(4\pi G)$, for the self-interaction coupling λ and G the gravitational constant. In equation (3), we are using the units $\hbar = 1$,

for the reduced Planck's constant, and $c = 1$, for the speed of light; from hereafter we use these units. Notice that the self-interaction increases the critical mass for large values of the mass of the SF. In the context of standard axions, their masses run between 10^{-6} and 10^{-3} eV in order to account for the DM. The original QCD-axion has typical masses between keV and MeV and a coupling to standard matter and radiation was considered. Initially, it was expected that these particles could be observable in particle accelerators; however, at the time they have not been detected. Furthermore, cosmological observations suggest that they are ruled out (Hlozek et al. 2015). Masses of the so-called invisible axion run between 10^{-33} and 10^{-3} eV and nowadays the so-called standard axions have masses between 10^{-6} and 10^{-3} eV (Kim & Carosi 2010). The self-interaction is important in order to make these models to predict the correct big bang nucleosynthesis abundances of light elements at 1σ-confidence level (Li et al. 2014) and other cosmological observations (see e.g. Suárez & Chavanis 2015). For ultra-light SFs, even the free scalar is observationally appealing since the critical mass is close, in order of magnitude, to that of observed SMBHs; however, the self-interaction in this case plays an important role since it helps to predict critical masses around $10^{12}\,\mathrm{M}_\odot$ for larger masses of the SF. Recently, Chavanis (2016) studied analytically, in the Newtonian approximation, the collapse of self-interacting BECs with attractive self-interaction in the Thomas–Fermi limit (dominant self-interactions regime), and found the critical mass and time of collapse of a BEC to form a BH. In the context of the 'standard' axion mass ($m \sim 10^{-4}$ eV), the formation of mini BHs with masses $M \sim 10^{-13}\,\mathrm{M}_\odot$ is predicted. For ultra-light axions ($m \sim 10^{-20}$ eV), it is predicted that BHs with masses of $M \sim 10^5\,\mathrm{M}_\odot$ are formed (the BH at the centre of the Milky Way is $\sim 10^6\,\mathrm{M}_\odot$), with reasonable times of collapse of Myr.

In what is concerning to this work, our simple model only considers the free field which is enough for our purposes. Nevertheless, we aim to extend our approach in future works.

3 BLACK HOLES WIGS AS LONG-LASTING DARK MATTER HALOES

Besides the problem of formation of an SMBH through the collapse of SFDM configurations, a further question remains: Once the SMBH is formed, does a self-gravitating and stable scalar galactic halo remain? Strictly speaking, no-hair theorems lead us to give a negative answer to the question. However, for realistic circumstances and practical purposes, the answer is surprisingly affirmative. No-hair theorems condemn these solutions to pass away after some time (Bekenstein 1995; Gürlebeck 2015); while that is true, it also has been demonstrated that some solutions survive at least a cosmic time. That is, although BHs are condemn always to be bald, nothing prevent them to wear wigs along their whole life. The boson excitations making up the wigs are subject to gravity and also to their own dispersive nature inherit by the KG equation. Although a perfect balance between these competing effects cannot be achieved, at least the decay time can be controlled choosing a proper mass for the configuration. Barranco et al. (2011, 2012), and more recently Sanchis-Gual et al. (2017), studied analytically and numerically configurations of SF embedded in a Schwarzschild space–time, once the BH has been formed. They realized that it is possible to find physically meaningful, long-lived SF configurations. In particular, for ultra-light SFs laying around SMBHs and axions around primordial BHs. They found that for masses $m < 10^{-22}$ eV and SMBHs of $M < 5 \times 10^{10}\,\mathrm{M}_\odot$, the configurations can survive for times larger than 10^{10} yr. In this sense, their results strongly support the hypothesis that the DM is an SF in the galaxies hosting SMBHs. Furthermore, the whole dynamics of the system, including its formation and evolution along the cosmic history, arises from a single physical framework without aid of baryonic physics.

4 THE MODEL: ULTRA-LIGHT SCALAR FIELD CONFIGURATIONS IN A SCHWARZSCHILD SPACE–TIME

We start studying the simplest model for an SFDM halo hosting a BH. We assume that the geometry of the space–time surrounding a BH is described by the Schwarzschild metric which, in spherical coordinates, is given by

$$\mathrm{d}s^2 = -\left(1 - \frac{2M}{r}\right)\mathrm{d}t^2 + \left(1 - \frac{2M}{r}\right)^{-1}\mathrm{d}r^2 + r^2\mathrm{d}\Omega^2, \tag{5}$$

where M is the mass of the BH in units of distance (from hereafter we use units $G = 1$) and $\mathrm{d}\Omega^2 \equiv \mathrm{d}\theta^2 + \sin^2\theta\,\mathrm{d}\varphi^2$ is the solid angle square differential.

The dynamics of the SF described by the KG equation written in a Schwarzschild background space–time is given by

$$-\partial_t^2\phi + \frac{g}{r^2}\partial_r\left[r^2\, g\,\partial_r\phi\right] - g\frac{L_{\theta,\varphi}(\phi)}{r^2} - g\left(m^2 + \lambda\phi^2\right)\phi = 0, \tag{6}$$

where we have assumed $r \neq 2M$ to avoid singular points and we have introduced the following definitions of the angular-momentum operator and the g function:

$$L_{\theta,\varphi}(\phi) \equiv \frac{1}{\sin\theta}\partial_\theta\left(\sin\theta\,\partial_\theta\phi\right) + \frac{1}{\sin^2\theta}\partial_\varphi^2\phi; \tag{7}$$

$$g(r) \equiv \left(1 - \frac{2M}{r}\right). \tag{8}$$

It is easy to realize that equation (6) is a separable equation with respect to time and space coordinates. Thus, it admits solutions of the form

$$\phi(t, r, \theta, \varphi) = \psi(r, \theta, \varphi)\,\mathrm{e}^{-i\omega t}, \tag{9}$$

with harmonic time dependence for an arbitrary frequency ω. After plugging equation (9) into (6), we obtain

$$\left(\omega^2 - gm^2\right)\psi + \frac{g}{r^2}\partial_r\left[r^2 g\;\partial_r\psi\right] - g\frac{L_{\theta,\varphi}(\psi)}{r^2} - g\lambda\psi^3 = 0. \tag{10}$$

By the moment, in this work we set $\lambda = 0$ for sake of simplicity, in which case the last equation is linear and admits solutions of the form

$$\psi(r, \theta, \varphi) = R_l(r)\,Y_l^n(\theta, \varphi), \tag{11}$$

where R_l is a function depending only on the radial coordinate r and the angular solution is given by the spherical harmonics Y_l^n for non-negative integers $l \geq |n|$. After using equation (8), the radial equation is given by

$$m^2 R_l - \frac{g}{r^2}\partial_r\left[r^2\, g\;\partial_r R_l\right] + g\frac{l(l+1)}{r^2} - \frac{2\,Mm^2}{r}R_l = \omega_l^2 R_l, \tag{12}$$

where ω_l is the corresponding frequency for the solution with the integer l. Notice that the last term on the left-hand side in equation (12) becomes small far away from the BH's event horizon. In the case

Table 1. Maximum wavenumbers, $k^{\max}$, and minimum characteristic lengths, $r_s^{\min}$, of a single state solution of the SF of mass $m = 10^{-22}$ eV, for a range of parameters including typical observational masses of SMBHs. Quasi-bound states of the system have square frequencies laying in the resonance band $(V_{\rm eff}(x^{\min}), m^2)$.

$M/M_\odot$	α	$k^{\max}/m$	$r_s^{\min}$/kpc
10^7	10^{-6}	8.8×10^{-4}	1.14
10^8	10^{-5}	2×10^{-3}	0.25
10^9	10^{-4}	6×10^{-3}	0.083
10^{10}	10^{-3}	2×10^{-2}	0.025
1.2×10^{10}	2.5×10^{-3}	3×10^{-2}	0.017
2.5×10^{10}	5×10^{-3}	4×10^{-2}	0.013
5×10^{10}	7.5×10^{-3}	5×10^{-2}	0.010

$2Mm^2/r \to 0$, equation (12) turns into the free Schrodinger equation. This last point is rather important in what follows. The length-scale $2Mm^2$ shall turn out to be a natural measure of the size of the configuration. Even though the scale of the BH is very different to that at which the galactic dynamics occurs, masses M for SMBHs give rise to $2Mm^2 \sim$ kpc. Moreover, since we are interested in describing the phenomenology occurring inside the central region of the DM halo, close to its edge at scales of few kpc, solutions of equation (12) in the regime where $r > 2Mm^2$ are actually what we are looking for. In the following sections, we are going to handle equation (12) in such a limit. Before doing so, we shall stop to analyse the spectrum of solutions arising for the range of parameters relevant for SMBHs.

4.1 About the eigenvalue problem for the Schwarzschild–Klein–Gordon system

For given masses of the SF and the BH, the spectrum of solutions has been determined numerically and semi-analytically in Barranco et al. (2011, 2012). In these works, the authors follow a standard procedure: they use convenient radial coordinates, so the KG equation can be transformed into a Schrodinger-like equation with a corresponding effective potential. They demonstrate that the frequencies of the solution cannot be larger than the depth of the well-potential (which is dubbed as 'resonance band'). Besides, this is equivalent to the standard procedure of solving the Schrodinger equation analytically and to use boundary conditions to determine the full spectrum allowed at each physical setup. A similar analysis can be done by analysing the KG equation with parameters in a range of values corresponding to models for galactic haloes. Here, we follow such a procedure, including realistic values of the parameter $\alpha \equiv Mm$, corresponding to realistic masses of SMBHs which run between 10^6 and $10^{10}\,M_\odot$ (McConnell & Ma 2013; Larkin & McLaughlin 2016) and assuming a mass of the SF $m = 10^{-22}$ eV (see Table 1).

For convenience, we can pick coordinates such that equation (12) takes a fully hyperbolic form; in the radial case we use the Regge–Wheeler tortoise coordinate defined as $r^* \equiv r + 2M\ln(r/2M - 1)$, such that (12) can be written as

$$-\partial^2_{r^*} Q^l + V_{\rm eff} Q^l = \omega_l^2 Q^l, \tag{13}$$

where $Q^l \equiv rR^l$, and we have introduced an effective potential given by

$$V_{\rm eff}(r; l, m, r_s) \equiv g(r)\left[m^2 + \frac{l(l+1)}{r^2} + \frac{2M}{r^3}\right]. \tag{14}$$

By solving exactly the eigenvalue problem established by equation (13), we would be able to determine the full spectrum of solutions allowed for this setup. However, in real galaxies, the SFDM halo coexists with stars and gas that might modify considerably the features of the system. For that reason, and for simplicity, we consider it is reasonable to set the characteristic length r_s of the solution as a free parameter, defined as the inverse of the wavenumber k, i.e. $r_s \equiv 1/k$ (with $k^2 \equiv \omega^2 - m^2$), and to determine an upper cut-off for k, denoted by $k^{\max}$ (see Table 1). Let us now consider the spherically symmetric case with $l = 0$. For $m = 10^{-22}$ eV, the potential wells for realistic cases are quite shallow (as shown in Table 1 and Fig. 1). As a consequence, even for the most massive BH observed so far, the resonance band is pretty narrow. This suggests that the spectrum of solutions is almost empty for the lightest BHs, and hence such solutions can be approximated as a single state with $\omega \sim m$, as assumed (see also Ureña-López & Liddle 2002).

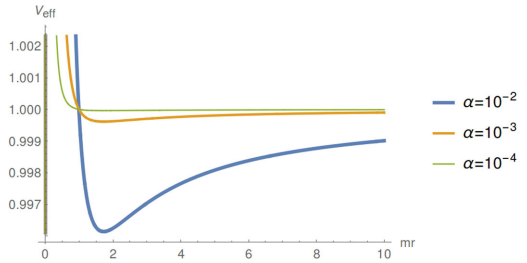

Figure 1. The effective potential for the general Schwarzschild–Klein–Gordon equation for different values of the parameter α. For configurations to form DM haloes hosting SMBHs, smaller values of α should be considered, and pretty shallow potentials arise. As a consequence, very large characteristic lengths r_s are expected, which is in agreement, in order of magnitude, with other values of r_s obtained from fits to rotation curves of galaxies (see e.g. Bernal et al. 2017a).

According to Barranco et al. (2011, 2012), stationary modes with real frequencies $\omega^2 > m^2$ do not exist. They found that the spectrum of solutions is continuous. The previous statement is in agreement with no-hair theorems. Furthermore, these modes do not decay at spatial infinity. If $0 < \omega^2 < m^2$, then the modes have purely imaginary frequencies and they form a discrete set for which the amplitude inside the potential-well takes very large values when compared with the amplitude close to the horizon; for that reason they are called *stationary resonances* within the band $V_{\rm eff} < \omega^2 < m^2$. When the conditions of no-waves coming from the horizon and the requirement of spatial infinity decay are imposed, the spectrum of stationary resonances become discrete and complex. This set of solutions has been called *quasi-resonances* in the literature (Ohashi & Sakagami 2004). Unfortunately, both sorts of solutions are non-physical due to the conserved energy density corresponding to a Killing vector, which diverges at the horizon. Nevertheless, from numerical calculations, Barranco et al. (2011) found healthier solutions dubbed as *dynamical resonances* with finite energy density in all regions. These solutions are damped oscillations driven by the BH and survive for very long times. The spectrum of such sort of solutions is the same than the stationary resonances. Actually, Barranco et al. (2012) showed that the real part of the frequency of the quasi-resonant modes coincides with the frequency of oscillation of the stationary and dynamical resonances, and the imaginary part coincides with the decay rate of the dynamical resonances. Now, since within this scenario it is assumed that SMBHs are surrounded by quasi-resonances that are as long-lived as the Universe, we can assume they are stationary and then we can, as a first approximation, neglect the decaying part of the solution controlled by the imaginary part of the frequencies. In principle, k could be taken as a free parameter, however we argue that the range of its

values is restricted by α. As mentioned above, k is allowed to take values below $k^{\max}$. Because α takes such small values for typical galactic SMBH masses, the characteristic length is expected to be quite large.

Usually, within the models accounting for SFDM configurations as galactic haloes, the values for k run between 0.35 and 10 kpc^{-1} (Robles, Martinez-Medina & Matos 2015; Bernal et al. 2017a). As we shall see below, the presence of a BH produces a considerate reduction in the size of the halo compared to fits of SFDM models without BH.

4.2 The SFDM configuration far away from the black hole

In the following we aim to study the behaviour of matter at regions far away from the BH, thus we need to solve equation (12) in the limit in which $2M/r \to 0$, that is

$$k_l^2 R_l + \frac{1}{r^2}\partial_r\left[r^2\,\partial_r R_l\right] - \frac{l(l+1)}{r^2} + \frac{2Mm^2}{r}R_l = 0. \tag{15}$$

This equation is valid for most of the central region of the SFDM halo. It must be stressed that the evolution of the SMBH and the galactic system lay in very different spatial scales. Even stars living in the deepest galactic regions, well inside the central halo, are parsecs away from the centre, while the Schwarzschild radius of the SMBH is one part in a million smaller. On one hand, $2M \sim 10^{-14}$ pc for a solar mass and $2M \sim 10^{-6}$ pc for an SMBH with $M \sim 10^{10}\,\mathrm{M}_\odot$. On the other hand, typically the size of the central halo runs from 1 to 10 kpc.

By taking again the change of variable $Q_l \equiv r R_l$, equation (15) becomes

$$\partial_{rr} Q_l + k^2 Q_l - \frac{l(l+1)}{r} + \frac{2Mm^2}{r}Q_l = 0. \tag{16}$$

For $l = 0$, which is sufficient for the spherically symmetric case, a solution is given by

$$\psi(r) = \psi_0\, \mathrm{e}^{-ikr}\, {}_1F_1\left(1 - i\frac{Mm^2}{k}, 2, i2kr\right), \tag{17}$$

where ψ_0 is a constant and ${}_1F_1$ is the hyper-geometric function of order (1,1). From now on we shall refer to linear combinations of this sort of solutions as SSFDM configurations. We shall analyse the features of the profiles arisen from this solution in detail in Section 6. Well inside the central halo it happens that $kr \ll 1$, therefore the solution approximates to

$$\psi \simeq \psi_0\,(1 - Mm^2 r) + \mathcal{O}[(kr)^2] + \mathcal{O}[(Mm^2)^2]. \tag{18}$$

This profile is in agreement to that proposed in Lee et al. (2015). For small radii inside the central halo, i.e. for $r \ll r_\mathrm{s}$, still far away from the BH ($2M \ll r$), the profile remains constant. Still inside the halo but closer to its edge ($r \sim r_\mathrm{s}$), the profiles start decaying. In the next section we will show that the BH produces a driving effect on the SF halo solution, and the more massive it is more cuspy is the profile of the halo.

5 THE DRIVING EFFECT OF THE BLACK HOLE ON THE HALO SOLUTION

Although equation (12) can be solved exactly and analytically, in this section we treat the problem perturbatively in order to have a more intuitive understanding of the effect that a BH exerts on to a bare SFDM solution. From equation (12), it can be noticed that the last term on the left-hand side is actually a perturbation to the KG

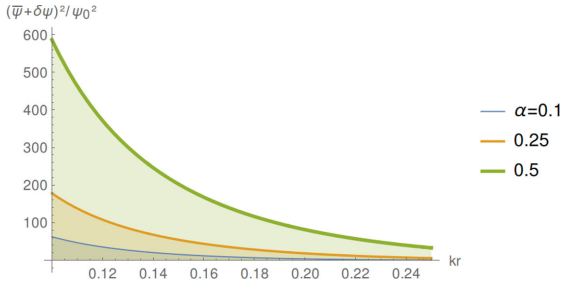

Figure 2. Dimensionless solutions of the SF perturbed by a BH for different values of the α parameter. As the mass of the BH increases, the solution becomes more cuspy and its width decreases. This effect is produced by a driving force due to the presence of the BH.

equation in flat space for a region $r \gg 2M$. Thus, we can split the SF into a bare solution plus a small perturbation induced by the BH:

$$\psi = \bar\psi + \delta\psi + \mathcal{O}(M^2), \tag{19}$$

being $\bar\psi$ the solution for the halo in flat space–time given by (Robles & Matos 2013b)

$$\bar\psi(r) = \bar\psi_0 \frac{\sin(kr)}{kr}, \tag{20}$$

which is an exact solution of the KG equation for an SFDM perturbation that corresponds to the galactic DM halo in the Newtonian limit found in the case of a temperature-corrected SF potential for $T \simeq 0$. The corresponding density profile coming from the linear combination of solution (20) for different values of k and $\bar\psi_0$ is dubbed as 'multistate SFDM' and it has been proved to be successful in fitting the rotation curves of galaxies (Robles & Matos 2013b; Bernal et al. 2017a), the velocity dispersions observed in dwarf spheroidal galaxies (Martinez-Medina et al. 2015), the strong gravitational lensing (Robles & Matos 2013a), and the dynamical masses from X-ray observations of galaxy clusters (Bernal et al. 2017b).

By plugging equation (19) with solution (20) into (15), and setting $l = 0$, we obtain an ordinary differential equation for the perturbation given by

$$\delta R_{,rr} + k^2 \delta R = -\bar\psi_0 \frac{r_0}{r}\frac{\sin\left[(k + \mathrm{d}k)r\right]}{r}, \tag{21}$$

that corresponds to a driven harmonic oscillator. Notice that the mass of the BH quantifies the amplitude of the external force which has the same functional form than the bare solution and has a wavenumber $k + \mathrm{d}k$; $\mathrm{d}k$ quantifies the closeness to the natural frequency of the oscillator: when $\mathrm{d}k \to 0$, the corresponding solution is in resonance with the external force and its amplitude is enhanced. Equation (21) holds the following analytic solution:

$$\psi_1^k = \bar\psi_1^k \left(\frac{m}{k}\right)^2 \left(\frac{r_\mathrm{s}}{r}\right)\left(Ci^{(-)}\cos kr - Si^{(+)}\sin kr\right), \tag{22}$$

where $Ci^{(-)} \equiv Ci[\mathrm{d}k\, r] - Ci[(k + \mathrm{d}k)\, r]$ and $Si^{(+)} \equiv Si[\mathrm{d}k\, r] + Si[(k + \mathrm{d}k)\, r]$ are the cosine and sine integral functions, respectively. From the behaviour of the $Ci^{(-)}$ and $Si^{(+)}$ functions, some physical information about the resonant solution can be extracted. First, the bigger the mass of the BH is, the solution for the SF becomes more cuspy (see Fig. 2). As expected, when the frequency of the oscillator is equal to that of the driving force, the amplitude of the oscillator blows up. This happens because we are considering an idealized situation in which the driving force is formed by a single state of the bare solution; however, a more realistic configuration would correspond to a driven force as a coherent package made of

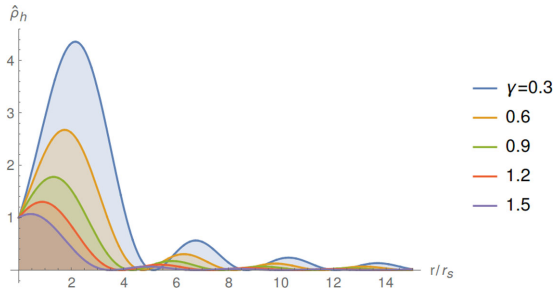

Figure 3. Dimensionless radial density profile for the SF configuration for different values of the parameter $\gamma \equiv m^2 M r_s$. The configuration takes its peak closer to the galactic centre as its characteristic size r_s increases for a fixed value of the BH mass M.

multiple bare solutions with different frequencies, laying within a frequency band of width dk. In such case, dk would never vanish and therefore the solution for the oscillator would never be purely resonant; in turn, while the driving force becomes narrower, the amplitude increases without blowing up. None the less, for the purposes of this subsection, the idealized situation is enough to realize that the perturbative term due to the presence of a BH works as a driving force which produces enhancement of the amplitude of the solution of the SF. Fig. 2 shows solutions in this simple case with d$k \ll 1$ for different masses of the BH.

6 DARK MATTER MASS AND DENSITY PROFILES

As mentioned above, in this work we model the central region of an SFDM halo housing an SMBH. We assume that the observer is placed in a region far away from the BH in a radius smaller than the characteristic size of the halo; in such regime, the back-reaction of the BH and scalar DM can be neglected. We model such a system by assuming that DM is described by a configuration of a complex SF laying in a Schwarzschild space–time. This framework is valid in the quasi-static limit in which the BH is already formed and it remains still without accreting any matter or gas. Within this regime, the velocity field of matter is affected by the BH presence only by means of the halo solution given by

$$\rho_{\rm dm} \equiv \phi\, \phi^* = \rho_{\rm s} \left| {}_1F_1\left(1 - \frac{i\alpha m r_{\rm s}}{2}, 2, i2x\right)\right|^2, \tag{23}$$

where the central density $\rho_{\rm s}$ is a free parameter and we have defined the dimensionless variable $x \equiv kr = r/r_{\rm s}$. It is interesting to notice that the order of magnitude of the parameters involved in the solution naturally coincides with typical sizes of cores in observed galaxies: for an ultra-light SF with mass $m \sim 10^{-22}$ eV we have $m^{-1} \sim 0.5$ pc (using proper units $\hbar = c = 1$) and for a BH with mass $M \sim 10^{10}\,{\rm M}_\odot$, $(Mm^2)^{-1} \sim$ kpc. Taking advantage of these scaling relations, we choose the following parametrization for the characteristic length $r_{\rm s}$ of the solution:

$$r_{\rm s} = \frac{\gamma}{\alpha m}, \tag{24}$$

where we introduced γ as free parameter that scales $r_{\rm s}$ in units of $(Mm^2)^{-1}$. Using this parametrization, the dimensionless SSFDM density of the SF configuration reads as

$$\hat{\rho}_{\rm dm}(x;\gamma) \equiv \frac{\rho_{\rm dm}(x;\gamma)}{\rho_{\rm s}} = \left| {}_1F_1\left(1 - \frac{i\gamma}{2}, 2, i2x\right)\right|^2, \tag{25}$$

that we show in Fig. 3 for different values of γ. In this way, we define conveniently the dimensionless DM density profile as a function of the dimensionless variable x, parametrized with a single free parameter γ.

As it can be seen in Fig. 3, as γ increases, the point where the density profile maximizes, $r_{\rm max}$, shifts apart from the centre. Therefore, below such radius DM is not as dense as in an intermediate region. This can be interpreted as follows: an initially core-like profile of DM turns into a dough-nut-like configuration when it interacts with a relativistic particle placed at the centre. This suggests that the largest amount of DM does not concentrate at the centre. At this point, we have not determined the value of the central density, thus we cannot quantify the mass of DM. None the less, we can imply there is a region off the centre of the galactic disc concentrating more DM than in the centre for a fixed value of $r_{\rm s}$.

From integrating out the density profile (25) within a given radius, we obtain the radial mass density profile for the halo as

$$M_{\rm dm}(r) = \int_0^r \rho_{\rm dm}(r) r^2 {\rm d}r = r_{\rm s}^3 \rho_{\rm s} \hat{M}_{\rm dm}(x), \tag{26}$$

where we have defined the dimensionless mass profile as

$$\hat{M}_{\rm dm}(x) \equiv \int_0^{r/r_{\rm s}} \hat{\rho}_{\rm dm}(x)\, x^2 {\rm d}x. \tag{27}$$

At this point, the only information we have about the values of the free parameters of these profiles, $r_{\rm s}$ and $\rho_{\rm s}$ (or alternatively $\rho_{\rm s}$ and γ), has been extracted from the condition of the existence of bound solutions in the KG equation determined by the structure of the effective potential (14). As a consequence, a lower bound for $r_{\rm s}$ is established by boundary conditions, which is in agreement with results from Lee et al. (2015):

$$\rho_{\rm s} \sim \alpha. \tag{28}$$

However, the remaining indetermination is going to be removed by using information from some universal features of galaxies. In the next sections, we shall reduce the space of parameters of our model by imposing a relation between the value of the central SFDM density and γ. We achieve this by assuming the universal maximal acceleration (UMA) of DM particles, recently reported in Ureña-López et al. (2017). In Section 8, in order to have a rough estimate of $r_{\rm s}$, we use the observed correlation between the mass of the BH and the velocity dispersion of baryonic matter in galaxies.

7 CONSTRAINT ON THE CENTRAL DM DENSITY FROM THE MASS DISCREPANCY–ACCELERATION RELATION

Recently, it has been shown from the observed rotation curves of 153 galaxies from the SPARC (Spitzer Photometry & Accurate Rotation Curves) data base (Lelli, McGaugh & Schombert 2016), including galaxies with very different features and morphologies with high-resolution gas and stars information, that the acceleration inferred from the observations strongly correlates with the acceleration due to the baryonic matter, showing a mass discrepancy at the value $g\dagger = 1.2 \times 10^{-10}\,{\rm m\,s^{-2}}$ (McGaugh et al. 2016; Lelli et al. 2017). Such MDAR can be interpreted as a correlation between the baryonic and the DM, and moreover, the maximum radial acceleration purely produced by baryonic matter and that of DM are closely related, and in the case that DM particles exist, the maximum radial acceleration they can reach in all haloes, $g_{\rm dm}$, cannot be greater than the UMA value given by (Ureña-López et al. 2017)

$$g_{\rm dm}^{\rm max} = 0.65 g^\dagger = 7.8 \times 10^{-11}\,{\rm m\,s^{-2}}. \tag{29}$$

On the other hand, the acceleration profile comes as a theoretical prediction for every model and its maximum value should be restricted by the last value. In our case, specific values of the parameter ρ_s for the SF density profile (23) (given a mass M of the BH) are required in order to predict the UMA value (29). The modulus of the radial acceleration profile for the bosons forming the halo can be computed in terms of the mass profile as follows:

$$g_{\rm dm}(r;\gamma,\alpha) = \frac{G M_{\rm dm}(r;\gamma,\alpha)}{r^2}, \tag{30}$$

which in terms of the dimensionless mass profile (27) and the dimensionless independent variable x can be easily rewritten as

$$\begin{aligned} g_{\rm dm}(r;\gamma,\alpha) &= G\, r_s \rho_s \frac{\hat{M}_{\rm dm}(x)}{x^2}, \\ &= G\, \mu_{\rm dm}\, \hat{g}_{\rm dm}(x;\gamma), \end{aligned} \tag{31}$$

where we have defined the dimensionless acceleration profile as

$$\hat{g}_{\rm dm}(x;\gamma) \equiv \frac{\hat{M}_{\rm dm}(x;\gamma)}{x^2}, \tag{32}$$

and we used the surface density definition given in Ureña-López et al. (2017):

$$\mu_{\rm dm} \equiv r_s \rho_s. \tag{33}$$

By imposing the constraint (29) over the theoretical maximum of the acceleration profile, we obtain a value for the halo's central surface density given by

$$\mu_{\rm dm} = \frac{0.65 g^\dagger}{G\, \hat{g}^{\rm max}_{\rm dm}(\gamma)}, \tag{34}$$

and consequently the central value for the density profile is

$$\rho_s = \alpha \frac{\rho^\dagger}{\gamma\, \hat{g}^{\rm max}_{\rm dm}(\gamma)}, \tag{35}$$

where

$$\rho^\dagger = \frac{0.65\, m\, g^\dagger}{G} = 0.807 \times 10^3 \frac{\rm M_\odot}{\rm pc^3}. \tag{36}$$

for $m = 10^{-22}$ eV. Notice that relation (35) is consistent with the boundary condition (28).

In Ureña-López et al. (2017), using the UMA value for DM profiles, solutions of the Schrodinger–Poisson system (valid at the Newtonian limit only), they conclude that the central surface density $\mu_{\rm dm}$ is a universal constant. In the context of the ultra-light SFDM model, for the so-called fuzzy or wave DM (WaveDM) soliton profile (Schive et al. 2014), $\mu_{\rm dm} = 648\, {\rm M_\odot\ pc^{-2}}$. This result brings as a consequence that the WaveDM soliton profile should be a universal feature of the SFDM haloes. However, in the context of this work, where central BHs in galaxies manifestly affect the DM profile in the core and also the central density, while it is true that $g^{\rm max}_{\rm dm}$ is a constant, from equation (34) it is clear that the central density $\mu_{\rm dm}$ is not necessarily constant. Rather, it obeys the following implicit relation between ρ_s and r_s:

$$r_s \rho_s - \mu_{\rm dm}(\gamma \equiv M m^2 r_s) = 0. \tag{37}$$

Therefore, the universality of the WaveDM soliton profile for galaxies hosting an SMBH not necessarily holds unless $M m^2 r_s =$ constant. Two interesting points arise from this last conclusion: First, haloes of galaxies with not-too-massive BHs in their centres nearly satisfy $M m^2 r_s = 1$. This can be realized using the analysis made in Section 4.1, where we saw that for small masses $k \to 0$, the SF profile can be described by the Ureña-Liddle solution (Ureña-López & Liddle 2002), for which r_s can be read off as $(Mm^2)^{-1}$. Secondly, assuming the UMA value (29) actually holds, in the case of observing galaxies that violate the universal WaveDM soliton profile, variations to the constraint (37) can be owed either (i) to the influence of baryons on the solitonic halo through gravity or (ii) to the influence of an SMBH at the centre of such galaxies. Consider we were studying the features of an SDFM halo for an specific galaxy and from fits of its rotation curve, or another observation, it turns out that $\mu_{\rm dm}$ differs from the universal value proposed in Ureña-López et al. (2017); therefore, we could set as a possibility the existence of a BH at its centre and, from the inferred value of $\mu_{\rm dm}$, the mass of the BH can be estimated.

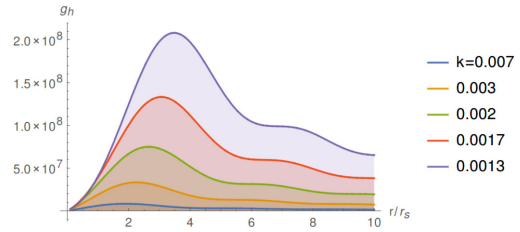

Figure 4. For a fixed mass of the BH $M \sim 10^{10}\, {\rm M_\odot}$, the radial acceleration profile $g_{\rm dm}(\gamma(k))$ is plotted for different wavenumbers k of the solution.

In order to completely fix the central density of our SFDM profiles we still need to fix r_s (or γ). In Section 8, we shall determine r_s by fitting the observed correlation between the mass of the BH and the velocity dispersion of baryonic matter inside the stellar bulge (see e.g. Ferrarese & Merritt 2000). However, at this point, we are able to set some restrictions over ρ_s from theoretical grounds. The following subsection is devoted to that purpose.

7.1 Theoretical upper bound for the central density of the SFDM configuration

In Section 4.1, we derived an upper bound for the wavenumber k of the solutions of the Schwarzschild–Klein–Gordon system, for a range of values of the BH mass (see Table 1). Here, we derive the values of the central SSFDM density profile from the UMA constraint (29), by using the procedure explained at the beginning of Section 7.

For a fixed value of the mass of the BH, M, the theoretical radial acceleration strongly depends on r_s (or k), as Fig. 4 shows. As the value of k increases, $g^{\rm max}_{\rm dm}$ decreases, and together with equation (35), we can see that $\rho_s(\alpha, \gamma(k^{\rm max}))$ increases. Therefore, for a fixed M, the value $\rho_s(\alpha, \gamma(k^{\rm max}))$ is an upper bound for all its possible values.

Let us denote such maximum value for the central density as $\rho^\alpha_{\rm max} \equiv \rho_{\rm dm}(x=0; \gamma = M m^2 r_s^{\rm min})$ in order to distinguish these values purely associated with theoretical quantities from those corresponding to a generic r_s, which are going to be inferred from observations later. The top panel of Fig. 5 shows the correlation between the parameter α (that quantifies the mass of the BH for a fixed mass of the SF) and its corresponding central density for the minimal value of r_s allowed. According to this relation, the intuitive and ideal picture drawn in Section 5 is correct: the larger the mass of the central BH is, the denser is the surrounding SF configuration (see the bottom panel of Fig. 5). This would be actually true if nature would choose $r_s^{\rm min} = 1/k^{\rm max}$; however, the complexity of baryons in real galaxies is mostly likely to mess up such assumption. None the

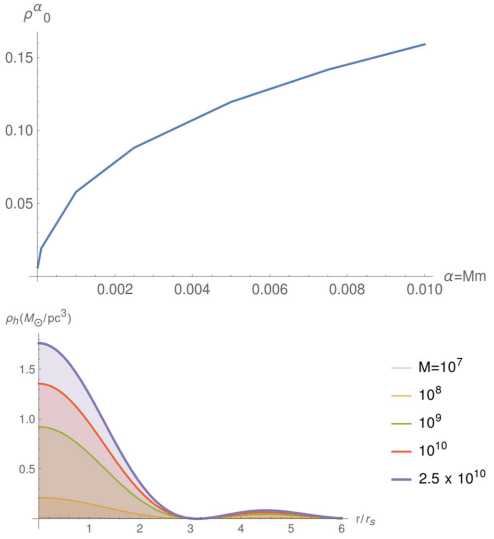

Figure 5. Top panel: Upper bounds for the central density values $\rho^{\alpha}{}_{\max}$ as function of the mass M of the BH. These values are obtained for SF profiles fixing the characteristic length as $r_{\rm s}^{\min} = 1/k^{\max}$. Bottom panel: Density profiles for different values of M and $r_{\rm s}^{\min}(M)$. As expected, the halo is denser at the centre for more massive BHs; effectively, the BH increases the height and shrinks the length of the SF profile. This is in agreement with results from our toy model discussed in Section 5.

less, it gives us an idea of how the haloes would ideally be without baryons, also it sets up some restrictions over the central density.

8 KINEMATICS OF VISIBLE MATTER INSIDE THE GRAVITATIONAL POTENTIAL OF THE SFDM HALO

In practice, the mass of a BH is derived from measurements of different features of the velocity field of stars and gas moving along the gravitational well-potential produced by the whole system formed by the DM halo, stars, gas, and the BH. From theoretical grounds, the procedure goes the other way round: we assume a BH fully specified by its mass and we derive some kinematic features of the velocity field of the system. In this section, our goal is to give an estimate for the free parameters of our SFDM model in concordance with some observational features of galaxies. This shall serve us to test at which extent our formalism is capable to describe the central regions of haloes laying in a space–time considerably influenced by the presence of an SMBH. As a first step, we shall use the UMA constraint (29) (Ureña-López et al. 2017) to reduce the space of parameters. Similarly as we did at theoretical level in Section 7.1 by bounding the values of the central density, the UMA constraint provides a relation between $\rho_{\rm s}$ and $r_{\rm s}$. As a second step, in order to obtain an estimate of the remaining free parameter $r_{\rm s}$, we compute the baryonic stellar velocity dispersion by solving the Jeans equation for different values of the mass of the BH. For each value of M, we derive an estimate of $r_{\rm s}$ that gives rise to the target value of the velocity dispersion σ^* reported in McConnell & Ma (2013). We carry out such procedure in two cases:

(1) In Section 8.2, we assume that the gravitational pull of DM is dominant. We dub such case DMD. Here, the velocity dispersion of baryons only depends on the DM profile parameters and the ratio of $r_{\rm s}$ and the effective radius associated with the stellar density profile. In this idealized case, as a first result, we obtain a correlation between $r_{\rm s}$ and the mass of the BH. This allows us to derive, as a complementary result, the central surface density profile $\mu_{\rm dm}$ of DM as function of γ, which is a generalization of the main result from Ureña-López et al. (2017) for DMD galaxies hosting SMBHs. This idealized case may be applicable to UCD galaxies, which are claimed to possibly host SMBHs and it is assumed that they host a small amount of baryons, as inferred from their poor luminosities (Drinkwater et al. 2000; Ahn et al. 2017).

(2) In Section 8.3, we study the second case LGAL, in order to consider large galaxies. We consider that the gravitational influence of both baryons and DM described by the SSFDM model is important.[1] We must point out here that, since we are using a Schwarzschild geometry of space–time a priori, we are ignoring the feedback of baryons and the SF itself on the solution of the DM profile, and therefore the formalism used in these cases only provides a rough description of the system. However, the results are still useful to compare with other estimates arisen from similar models of DM within the regime of applicability, in order to figure out possible effects due to the presence of a BH.

In both cases, we consider an elliptical shape for the baryons distribution. In the second case, our formalism is valid to describe massive, dispersive and early-type galaxies and bulges of late-type galaxies. We take as cases of study specific real elliptical galaxies and bulges.

8.1 Visible matter in the galaxies and the Jeans equation

Because we are assuming spherical symmetry, our model predicts that stars only move along the radial direction. The stellar spatial distribution is fully described by the distribution function $f(r, v)$, which is the probability of finding a star at radius r with velocity v. This distribution satisfies the Boltzmann equation and once it is known, all the macroscopic statistical quantities associated with the visible part of the galaxy can be determined. However, to determine such distribution is not straightforward, and sometimes it is not even necessary to compute some observables, as it happens with the stellar velocity dispersions,[2] σ_*, which obey the Jeans equation. This relation can be derived from the Boltzmann equation in the case that stars in the system are non-collisional and when spherical symmetry is imposed, and is given by (Binney & Tremaine 2008)

$$\frac{1}{\rho_*(r)}\frac{{\rm d}(\rho_*\sigma_*^2)}{{\rm d}r} + \frac{2\beta\sigma_*^2}{r} = -\frac{GM_{\rm tot}(r)}{r^2}, \tag{38}$$

where ρ_* is the stellar density profile and β the anisotropy parameter that we shall ignore since, even in the more complex cases, it modifies the results no more than 5 per cent (Binney & Tremaine 2008; McConnell & Ma 2013). The total mass of the galactic system, $M_{\rm tot}$, is defined by

$$M_{\rm tot}(r) = M_{\rm bar}(r) + M_{\rm dm}(r), \tag{39}$$

where $M_{\rm bar}$ and $M_{\rm dm}$ are the mass of the baryons (gas and stars) and the DM, respectively, enclosed inside a given radius r. The left-hand side of equation (38) corresponds to kinematic terms of the visible matter, while the right-hand side involves the dynamical sources that produce the galactic well-potential that triggers the kinematics.

[1] We assume the gravitational influence of the BH only happens through the DM solution.

[2] The stellar velocity dispersion is defined as the square root of the standard deviation of the velocity probability distribution: $\sigma_*^2 \equiv \int_V f(x, v)(v - \bar{v})^2 {\rm d}^3x\, {\rm d}^3v$, where $\bar{v}$ is the mean radial velocity.

In this work, we assume $M_{\rm bar}$ can be described by the Plummer density profile, which is typically used to describe stars in galactic bulges, but also for elliptical and dwarf galaxies (see e.g. Walker et al. 2009). For this profile, the radial density distribution of stars is given by

$$\rho_*(r) = \frac{\rho_*^0}{\left[1+(r/R_{\rm eff})^2\right]^{5/2}}, \tag{40}$$

where $\rho_*^0 \equiv 3M_*^{\rm tot}/(4\pi R_{\rm eff}^3)$ is the stellar central density and $M_*^{\rm tot}$ is the mass of stars enclosed within the effective radius $R_{\rm eff}$, which is defined as the radius at which the luminosity of the galaxy decreases to a half of its central value. The corresponding Plummer mass profile M_* is obtained by integrating the density profile (40) within a radius r. The dimensionless Plummer mass profile of stars, $\hat{M}_*$, is defined as

$$\hat{M}_*(r) \equiv \frac{M_*(r)}{M_*^{\rm tot}} = \frac{(r/R_{\rm eff})^3}{\left[1+(r/R_{\rm eff})^2\right]^{3/2}}. \tag{41}$$

8.2 Determining the SSFDM characteristic length from the '*M–σ*' relation for the DMD case

The mass of visible matter in galaxies is an important parameter to consider in order to understand the co-evolution of the BH, the DM halo and the messy system of stars and gas. Real galaxies hosting SMBHs usually contain an important fraction of visible matter in-falling into the gravitational well-potential and, thanks to such component, these objects can be detected. In the next subsection, we shall take into consideration the gravitational contribution of baryons into the Jeans equation for very specific luminous galaxies. However, in this subsection, we start considering a simpler idealized case, that is, an hypothetical system where the gravitational well-potential is mainly produced by the SF configuration forming the DM halo.

Here, we model the baryonic distribution using the Plummer profile (40) assuming a spherical system. The parameters of this profile have been well tested and it can be used to model systems of different sizes and luminosities (Walker et al. 2009). As mentioned before, this case may be applied and tested in the future in UCD galaxies (Ahn et al. 2017). In this respect, we must to mention that, at the date, there is not enough information to realize whether UCDs are actually galaxies or compact clusters (Drinkwater et al. 2000). For that reason, not even information about the stellar kinematics is still available. Although this sort of systems need to be further investigated, at the moment we cannot exclude the possibility of the existence of these old galaxies. From the theoretical point of view (Barranco et al. 2011, 2012; Escorihuela-Tomas et al. 2017), it is reasonable to expect the existence of these systems at some point when all baryons have been accreted, let us recall that in these models DM decays much slower than baryons.

The Jeans equation (38) in this case reads

$$\frac{1}{\hat{\rho}_*(r)}\frac{{\rm d}(\hat{\rho}_*\sigma_*^2)}{{\rm d}r} = -\frac{GM_{\rm dm}(r)}{r^2}. \tag{42}$$

Notice that $M_*^{\rm tot}$ is not a free parameter any more. The last equation is equivalent to

$$\sigma_*^2(r) = \frac{1}{\hat{\rho}_*(r)}\int_0^r \frac{GM_{\rm dm}(r')\,\hat{\rho}_*(r')}{r'^2}\,{\rm d}r', \tag{43}$$

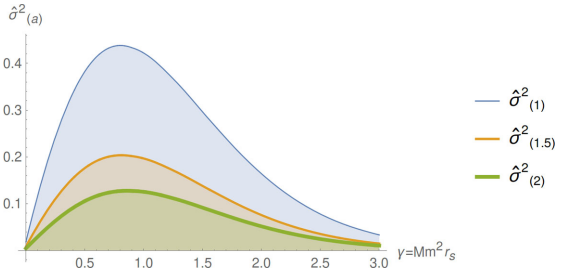

Figure 6. Dimensionless velocity dispersion $\sigma^2_{(a)}$ as function of γ for different values of a. If the size of the halo increases in relation to the size of the bulge, the velocity dispersion profile is suppressed.

where $\hat{\rho}_* \equiv \rho_*/\rho_*^0$. The last equation, written in terms of dimensionless quantities, turns into

$$\sigma_*^2(x) = \frac{G\,\rho^\dagger}{m^2\alpha}\frac{\gamma}{\hat{g}_{\rm dm}^{\rm max}(\gamma)}\frac{1}{\hat{\rho}_*(x,a)}\int_0^x \frac{\hat{M}_{\rm dm}(x',\gamma)\,\hat{\rho}_*(x',a)}{x'^2}\,{\rm d}x', \tag{44}$$

where we have redefined the Plummer profile in terms of the dark-to-visible-size ratio, $a \equiv r_{\rm s}/R_{\rm eff}$, as

$$\hat{\rho}_*(x,a) \equiv \frac{1}{\left(1+a^2x^2\right)^{5/2}}. \tag{45}$$

It is worth to notice that equation (44) results to be a product of a term depending only on γ and other only depending on α. The square of the stellar velocity dispersion evaluated in the effective radius is given by

$$\sigma_*^2(R_{\rm eff}) = \frac{(v^\dagger)^2}{\alpha}\,\sigma^2_{(a)}(\gamma), \tag{46}$$

where we have introduced the SF characteristic velocity $v^\dagger$ and the dimensionless quantity $\sigma^2_{(a)}(\gamma)$ depending on the value of a as

$$(v^\dagger)^2 \equiv \frac{0.65\,g^\dagger}{m} = 1.209\times10^6\ {\rm m^2\,s^{-2}}, \tag{47}$$

$$\sigma^2_{(a)}(\gamma) \equiv \frac{\gamma}{\hat{g}_{\rm dm}^{\rm max}(\gamma)}\frac{1}{\hat{\rho}_*(1/a)}\int_0^{1/a}\frac{G\hat{M}_{\rm dm}(x',\gamma)\,\hat{\rho}_*(x',a)}{x'^2}\,{\rm d}x'. \tag{48}$$

Notice that the square of the actual velocity dispersion is just a rescaling of equation (48) which exclusively depends on α and the mass of the SF, m. The last point is interesting because, unlike other observables, the dependences on α and m in $\sigma^2_{(a)}$ are separated and hence they are not degenerated. In Fig. 6, $\sigma^2_{(a)}$ is plotted for some values of the dark-to-visible-size ratio a, for a fixed mass M of the BH. Notice that as the size of the halo increases in relation to the size of the bulge, the whole velocity dispersion profile is suppressed. Now, as it can be noticed from the integral in equation (48), the stellar density profile serves as a weight of the radial acceleration profile therefore the larger a is, such weight becomes steeper and the integrand falls down at smaller radius. This suggest a connection between baryons and their hosting SSFDM haloes, this is, for fixed M and $R_{\rm eff}$, visible matter in galaxies is less dispersive if it is embedded in larger haloes. Besides, for a given M, visible matter has larger maximum velocity dispersions if the dark-to-visible matter ratio is smaller, as shown in Fig. 6. This means that, in this model, the presence of baryons in the central galactic region enhances the velocity dispersion of stars.

Let us turn to find the values of the characteristic size of the halo, $r_{\rm s}$, such that, for a given value of M, we can reproduce the value of

Table 2. Parameters for the M–σ_* relation for samples of different classes of galaxies.

Type	α	β
Early	8.07 ± 0.21	5.20 ± 0.36
Late	8.39 ± 0.06	5.06 ± 1.16
Full sample	8.32 ± 0.05	5.64 ± 0.32

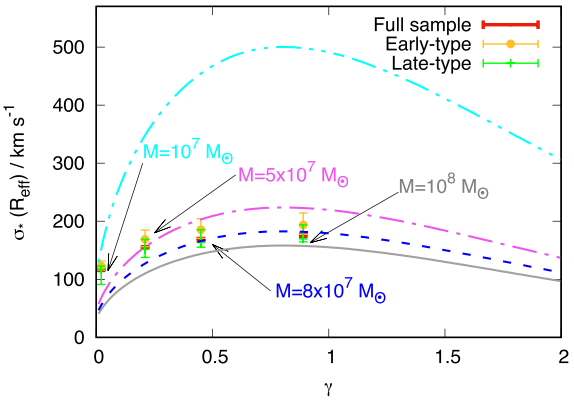

Figure 7. Lines correspond to theoretical γ–σ_* curves for different values of the BH mass: $M = 10^7\,\mathrm{M}_\odot$ (double-dot–dashed), $M = 5 \times 10^7\,\mathrm{M}_\odot$(dot–dashed), $M = 8 \times 10^7\,\mathrm{M}_\odot$ (dashed), and $M = 10^8\,\mathrm{M}_\odot$ (solid). The points with error bars correspond to picked values of γ that satisfy the phenomenological M–σ_* relation (49) for different samples of galaxies. Notice that the solid line corresponding to $10^8\,\mathrm{M}_\odot$ barely reaches the observed σ_* for the late-type sample.

σ_* given by the relation

$$\log_{10}\left(\frac{M}{\mathrm{M}_\odot}\right) = \alpha + \beta \log_{10}\left(\frac{\sigma_*}{200\ \mathrm{km\,s^{-1}}}\right). \quad (49)$$

The previous equation corresponds to the best fit of measurements of M and σ_* of a host of galaxies within three main samples: early- and late-type galaxies, and the full sample considering both types (McConnell & Ma 2013). The resulting parameters and errors of the M–σ_* relation for different samples are summarized in Table 2.

We constructed a set of bins of values of M running from 10^6 to $10^8\,\mathrm{M}_\odot$, and for each bin we use the prescription explained above to compute σ_* by solving equation (44). In our procedure we set $a = 1$, that is, $r_\mathrm{s} = R_\mathrm{eff} \sim$ kpc. We tried different values of γ and picked the one that best reproduced the value of σ_* associated with M by relation (49). Fig. 7 shows theoretical curves of σ_* as function of γ corresponding to different masses M of the BH; the points correspond to the picked values reproducing the observational value of σ_* along with the error bars corresponding to each sample. The resulting values of the characteristic length from this procedure are summarized in Fig. 8.

An important result of this subsection is that models with values of $a \geq 1$ fail to reproduce σ_* from equation (49) for masses $M > 10^8\,\mathrm{M}_\odot$; however, the results change for $a < 1$. This is important since it tells us that within the DMD model, only systems with $R_\mathrm{eff} > r_\mathrm{s}$ are able to reproduce the observed stellar velocity dispersion for a limited range of values of M. However, this scenario falls out of the regime of validity of DMD. Therefore, we can conclude that for DMD systems (with $a \geq 1$) the phenomenological σ_* can only be reached for BHs with masses up to $M \sim 10^8\,\mathrm{M}_\odot$ at most ($a = 1$) within the model, assuming that the gravitational field of DM is dominant (see Figs 7 and 9). Equivalently, this is consistent with the following: (i) large SMBHs live in visible-matter-dominated galaxies and (ii) in hypothetical DMD systems – like UCD galaxies might be – SMBHs could be found with masses of $M \sim 10^8\,\mathrm{M}_\odot$ at most.

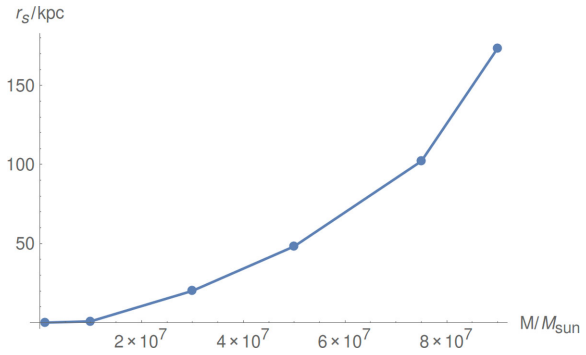

Figure 8. Scaling relation between the fit for γ characterizing the size of the SSFDM halo and the mass of the hosted SMBH for DMD systems. This relation is derived from fitting the observed M–σ_* relation.

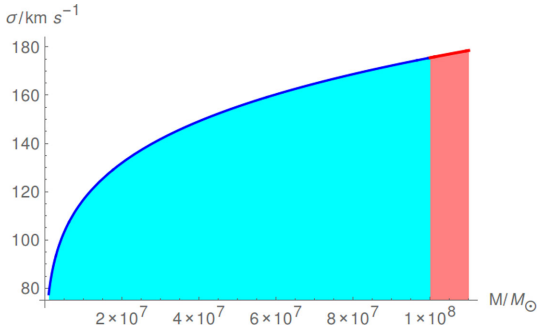

Figure 9. Empirical M–σ_* correlation (McConnell & Ma 2013) for a full sample of early- and late-types galaxies. The DMD regime within SSFDM can be only applied for SMBH with masses within the blue region.

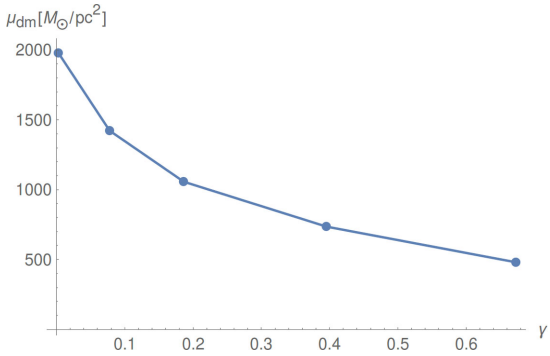

Figure 10. Surface density for several values of γ. As expected in this model, this quantity is not a constant, in contrast to that from SFDM models.

A complementary result of this work is the corresponding constraint (37) for values of r_s shown in Fig. 8. As mentioned before, unlike the standard SFDM profiles, in the case of SSFDM profiles μ_dm is not a constant, rather, as Fig. 10 shows, it depends on the parameter $\gamma = Mm^2 r_\mathrm{s}$. In SFDM models within the Newtonian regime, the constancy of μ_dm, along with some scaling relations of the parameters, bring up an important prediction for these models: the existence of a universal soliton-like profile in the central halo (Ureña-López et al. 2017). In satellite dwarf galaxies of the Milky Way, which are the closest to pure DM systems known at the date, this property would mean having a common mass around $10^7\mathrm{M}_\odot$ at

Table 3. This table summarizes some physical parameters of some representative galaxies and their SMBH and the derived values of the parameter r_s within SSFDM obtained from fitting the M–σ_* reported in ([a]) (McConnell & Ma 2013) and ([c]) (Larkin & McLaughlin 2016) (SMBH mass, total stellar mass, effective radius, characteristic size of the halo, and velocity dispersion). Values of $R_{\rm eff}$ labelled with 'b' were estimated using (50).

Galaxy	$M_{\rm BH}/{\rm M}_\odot$	$M_*^{\rm tot}/{\rm M}_\odot$	$R_{\rm eff}$/kpc	r_s/kpc	$\sigma(R_{\rm eff})/{\rm km\,s^{-1}}$
Milky Way bulge	4.1×10^6	9×10^9	1.4	0.615	103 ± 20^a
N3384	1.1×10^7	1.9×10^{10}	1.58^b	2.85	143.4 ± 7^a
N3585	3.2×10^8	1.6×10^{11}	5.2^b	2.1	213 ± 10^a
N3379	4.2×10^8	6.86×10^{10}	3.143^b	1.08	206 ± 10^a
M87	3.2×10^9	3.3×10^{11}	8.0	3.04	264 ± 13^c
M49	2.5×10^9	4.2×10^{11}	9.3	3.44	250 ± 13^c

300 pc which seems to have a strong observational support (Strigari et al. 2008). Here, when the influence of a BH on the DM profile is considered, the result of $\mu_{\rm dm}\neq$ constant implies that the soliton behaviour is altered and then the mass at $r\ll300$ pc is expected to be different depending on the mass of the guest BH.

8.3 Determining the SSFDM characteristic length from the '*M–σ*' relation for a sample of luminous galaxies

As mentioned above, in a similar way than for the previous case, in this subsection we aim to obtain estimates of the free parameters of the SSFDM profiles according to observations in the central regions of some large galaxies hosting SMBHs. Unlike Section 8.2, in which an idealized case is considered, here we model six real, luminous, and baryon-dominated galaxies (enlisted in Table 3). We refer this instance as LGAL, a case which technically differs from the DMD one studied in Section 8.2, since we take into consideration the full gravitational pull of baryons and DM into the Jeans equation. As mentioned above, although our models are far from being realistic approaches to the complex non-linear systems forming real large galaxies, the results in this subsection are obtained from observations from central galactic regions and it would be helpful to compare them with other estimates arisen in other SFDM models used to describe external galactic regions, like the multistate SFDM model (see e.g. Robles & Matos 2013b).

We solved numerically the equation (42) using the Plummer mass profile to model the visible matter contained in spherical systems and the mass profile corresponding to SSFDM described before for different elliptical galaxies hosting SMBHs in their centres. The corresponding parameters for each galaxy are enlisted in Table 3; they were extracted from catalogues in McConnell & Ma (2013) and Larkin & McLaughlin (2016). On the other hand, in Larkin & McLaughlin (2016), a correlation between the stellar total mass and the effective radius is reported and they infer the mean-stream trend in different galaxies by means of the following phenomenological relation:

$$R_{\rm eff}/{\rm kpc}=1.5\times\bar{M}^{0.1}(1+\bar{M}^5)^{0.1}, \tag{50}$$

where $\bar{M}\equiv M_*^{\rm tot}/2\times10^{10}\,{\rm M}_\odot$. We used this result in order to estimate the effective radius of some galaxies in our catalogue (Table 3) labelled with 'b'. Such table also summarizes the parameters used to solve the Jeans equation for each case.

After reducing the space of parameters using the UMA constraint derived in Section 7.1, we determined the characteristic length of the haloes corresponding to each galaxy in our catalogue such that, along with the other parameters of baryons in Table 3, the velocity dispersion σ_* from (49) is obtained. Once the set of points in the r_s–σ_* space were determined, a clear correlation between both parameters is observed which can be described by the following law:

$$\frac{\sigma_*(R_{\rm eff})}{{\rm km\,s^{-1}}}=109.0+38.4\times\left(\frac{r_s}{\rm kpc}\right). \tag{51}$$

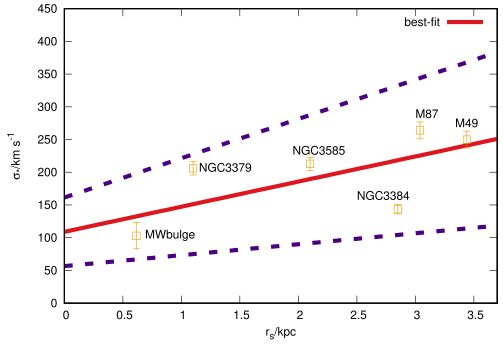

Figure 11. The solid line corresponds to the best fit of r_s–σ_* for the six galaxies in our catalogue given by the yellow points with their corresponding error bars (Table 3). The dashed lines correspond to the $\pm1\sigma$ theoretical errors from our best fit given by relation (51).

Fig. 11 illustrates the main result of this subsection: the observed velocity dispersion of baryons in centres of large and luminous galaxies like the Milky Way – which typically contain a dominant amount of baryons in those regions – cannot be produced only by gravitational potential wells of SSFDM haloes (as it has been shown in Section 8.2 as well), rather an important contribution of this wells should come from the baryons.

9 DISCUSSION AND CONCLUSIONS

In this paper, we assume the possibility that galactic systems hosting an SMBH in their centres were formed earlier in the Universe from the collapse of a BEC made of modes of an SF, most of them laying in the ground state. Based on previous studies from, e.g. Barranco et al. (2011, 2012) and Escorihuela-Tomas et al. (2017), we consider the hypothesis that the centres of DM haloes are made of quasi-resonant solutions of a real ultra-light SF that are being swallowed by the SMBH at such slow rate that their lifetime scales as the age of the Universe. Within the most general and realistic context, the SF would be self-interacting and self-gravitating and, along with the metric of space–time, form a complicated system of coupled non-linear differential equations which has been studied numerically by many groups since long time ago within some

range of applicability. However, the available computing and numerical tools at the moment have allowed to explore these systems in a range of parameters corresponding to models of boson stars at most and assuming some symmetries that wipe out some effects that should be present in more realistic models. Solutions for configurations of SF with the size of a galactic halo and BHs as massive as SMBH has not been obtained at the date in a general three dimensional space–time including all the possible effects.

In order to turn around such technical problem, in this paper we intent to construct a simple approach based in a semi-analytical procedure in order to model galactic systems in the quasi-static limit. As a first step towards addressing the problem, we propose the simplest prescription to describe DM in the centres of galactic systems hosting a central SMBH. We model the haloes of galaxies as configurations made of solutions of the KG equation with a Schwarzschild background. We find analytic solutions for a range of masses of the BH, M, in the limit $r > 2M$, that is, when the observer is placed far away from the BH and well within a radius smaller than the characteristic length of the SSFDM halo ($r < r_s$). In such regime, the back-reaction of the BH and SFDM can be neglected. By using such solutions we derive the corresponding density and mass profiles with ρ_s and r_s as free parameters, which were constrained using some observational features of galaxies. In specific, the space of parameters of the DM model was reduced by using the UMA constraint (Ureña-López et al. 2017). Later, the remaining free parameter r_s was fixed by fitting measurements of the velocity dispersion. In this procedure we considered two cases: First, DMD, an idealized case where it is assumed that the gravitational contribution of DM dominates the galactic potential well. The main result in this part is that it is possible to reproduce the observed stellar velocity dispersion at the effective radius of systems hosting SMBHs of at most 10^8 $M_\odot$. This hypothetical case could be used in the future to study UCD galaxies. However, our analysis in this case stands as theoretical so far, due to the lack of evidence and observational data regarding to these systems at the date.

Secondly, in the LGAL case we considered a sample of six real, large, and luminous galaxies hosting SMBHs and managed to reproduce their observed stellar velocity dispersions evaluated at the effective radius in every case. We realized in this case, that in the context of the SSFDM model, the role of gravity produced by baryons is crucial to reproduce the observed velocity dispersions. A complementary result of this work is a generalization of the constraint of $\mu_{\rm dm}$ derived in Ureña-López et al. (2017) for the case in which the galactic haloes host central SMBHs and it dominates the gravitational potential of the system. By reproducing the observational points of the M–σ_* relation, we derive a r_s–σ_* correlation in both cases. These results bring up new information about the SFDM model. It is worth to mention that given the recent direct observations of Sagittarius A by the EHT team (Ricarte & Dexter 2015; Eve 2015), a new era of detailed explorations of the deep-inner galactic region is about happening, this would bring up a new source of evidence of the properties of the SMBH and its influence on stars laying in the galactic bulge. Particularly, observations of the stellar evolution across this region will bring wealthy information of the DM configurations and it will be possible to discriminate between different DM models. Either to test our hypothesis about SMBH formation and to compare different DM models in the deep-inner galactic regions using these and upcoming direct observations of SMBHs in a short future is a compelling goal which we are after.

ACKNOWLEDGEMENTS

We thank the referee who reviewed the previous version carefully and help us to strengthen the results in this version. This work was partially supported by Consejo Nacional de Ciencia y Tecnología México under grants CB-2011 No. 166212, CB-2014-01 No. 240512, Project No. 269652, and Fronteras Project 281; Xiuhcoatl and Abacus clusters at Centro de Investigación y de Estudios Avanzados, Instituto Politécnico Nacional; I0101/131/07 C-234/07 of the Instituto Avanzado de Cosmología (IAC) collaboration (http://www.iac.edu.mx). AAA and LEP acknowledge financial support from CONACyT fellowships.

REFERENCES

Ahn C. P. et al., 2017, ApJ, 839, 72
Alcubierre M., Guzman F. S., Matos T., Nunez D., Urena-Lopez L. A., Wiederhold P., 2002a, in Klapdor-Kleingrothaus H. V., Viollier R. D., eds, Proc. 4th Heidelberg Int. Conf., DARK 2002, Dark Matter in Astro- and Particle Physics. Springer, Berlin, p. 356
Alcubierre M., Guzman F. S., Matos T., Nunez D., Urena-Lopez L. A., Wiederhold P., 2002b, Class. Quantum Gravity, 19, 5017
Amorisco N. C., Evans N. W., 2012, MNRAS, 419, 184
Arbey A., Lesgourgues J., Salati P., 2001, Phys. Rev. D, 64, 123528
Armengaud E., Palanque-Delabrouille N., Yèche C., Marsh D. J. E., Baur J., 2017, MNRAS, 471, 4606
Baldeschi M., Gelmini G., Ruffini R., 1983, Phys. Lett. B, 122, 221
Barranco J., Bernal A., Degollado J. C., Diez-Tejedor A., Megevand M., Alcubierre M., Núñez D., Sarbach O., 2011, Phys. Rev. D, 84, 083008
Barranco J., Bernal A., Degollado J. C., Diez-Tejedor A., Megevand M., Alcubierre M., Núñez D., Sarbach O., 2012, Phys. Rev. Lett., 109, 081102
Bekenstein J. D., 1995, Phys. Rev. D, 51, R6608
Bernal A., Matos T., Núñez D., 2008, Rev. Mex. Astron. Astrofis., 44, 149
Bernal A., Barranco J., Alic D., Palenzuela C., 2010, Phys. Rev. D, 81, 044031
Bernal T., Fernández-Hernández L. M., Matos T., Rodríguez-Meza M. A., 2017a, MNRAS, 475, 1447
Bernal T., Robles V. H., Matos T., 2017b, MNRAS, 468, 3135
Binney J., Tremaine S., 2008, Galactic Dynamics, 2nd edn. Princeton Univ. Press, Princeton, NJ
Böhmer C. G., Harko T., 2007, J. Cosmol. Astropart. Phys., 6, 025
Boylan-Kolchin M., Bullock J. S., Kaplinghat M., 2011, MNRAS, 415, L40
Bray H., 2010, preprint (arXiv:1004.4016)
Calabrese E., Spergel D. N., 2016, MNRAS, 460, 4397
Cappellari M., 2011, Nature, 480, 187
Caputi K. I. et al., 2015, ApJ, 810, 73
Chavanis P.-H., 2016, Phys. Rev. D, 94, 083007
Chen S.-R., Schive H.-Y., Chiueh T., 2017, MNRAS, 468, 1338
Colpi M., Shapiro S. L., Wasserman I., 1986, Phys. Rev. Lett., 57, 2485
Cruz-Osorio A., Guzmán F. S., Lora-Clavijo F. D., 2011, J. Cosmol. Astropart. Phys., 6, 029
de Blok W. J. G., 2010, Adv. Astron., 2010, 789293
de Blok W. J. G., McGaugh S. S., Bosma A., Rubin V. C., 2001, ApJ, 552, L23
Del Popolo A., Pace F., 2016, Ap&SS, 361, 162
Drinkwater M. J., Jones J. B., Gregg M. D., Phillipps S., 2000, PASA, 17, 227
Escorihuela-Tomas A., Sanchis-Gual N., Degollado J. C., Font J. A., 2017, Phys. Rev. D, 96, 024015
Ferrarese L., Ford H., 2005, Space Sci. Rev., 116, 523
Ferrarese L., Merritt D., 2000, ApJ, 539, L9
Gebhardt K. et al., 2000, ApJ, 539, L13
Genzel R. et al., 2017, Nature, 543, 397
González-Morales A. X., Marsh D. J. E., Peñarrubia J., Ureña-López L. A., 2017, MNRAS, 472, 1346

Goodman J., 2000, New Astron., 5, 103
Gürlebeck N., 2015, Phys. Rev. Lett., 114, 151102
Guzman F. S., Lora-Clavijo F. D., 2012, Phys. Rev. D, 85, 024036
Guzmán F. S., Ureña-López L. A., 2004, Phys. Rev. D, 69, 124033
Guzmán F. S., Ureña-López L. A., 2006, ApJ, 645, 814
Guzman F., Matos T., Villegas H., 1999, Astron. Nachr., 320, 9
Harko T., 2011, MNRAS, 413, 3095
Hawley S. H., Choptuik M. W., 2003, Phys. Rev. D, 67, 024010
Herdeiro C. A. R., Radu E., 2014, Phys. Rev. Lett., 112, 221101
Hidalgo J. C., De Santiago J., German G., Barbosa-Cendejas N., Ruiz-Luna W., 2017, Phys. Rev. D, 96, 063504
Hlozek R., Grin D., Marsh D. J. E., Ferreira P. G., 2015, Phys. Rev. D, 91, 103512
Hu W., Barkana R., Gruzinov A., 2000, Phys. Rev. Lett., 85, 1158
Hui L., Ostriker J. P., Tremaine S., Witten E., 2017, Phys. Rev. D, 95, 043541
Iršič V., Viel M., Haehnelt M. G., Bolton J. S., Becker G. D., 2017, Phys. Rev. Lett., 119, 031302
Ji S. U., Sin S. J., 1994, Phys. Rev. D, 50, 3655
Kim J. E., Carosi G., 2010, Rev. Mod. Phys., 82, 557
King A., 2016, MNRAS, 456, L109
Klypin A. A., Kravtsov A. V., Valenzuela O., Prada F., 1999, ApJ, 522, 82
Kroupa P. et al., 2010, A&A, 523, A32
Larkin A. C., McLaughlin D. E., 2016, MNRAS, 462, 1864
Lee J.-W., Koh I.-G., 1996, Phys. Rev. D, 53, 2236
Lee J.-W., Lee J., Kim H.-C., 2015, preprint (arXiv:1512.02351)
Lelli F., McGaugh S. S., Schombert J. M., 2016, AJ, 152, 157
Lelli F., McGaugh S. S., Schombert J. M., Pawlowski M. S., 2017, ApJ, 836, 152
Li B., Rindler-Daller T., Shapiro P. R., 2014, Phys. Rev. D, 89, 083536
Lundgren A. P., Bondarescu M., Bondarescu R., Balakrishna J., 2010, ApJ, 715, L35
Lynden-Bell D., 1969, Nature, 223, 690
Magaña J., Matos T., Suarez A., Sanchez-Salcedo F. J., 2012, J. Cosmol. Astropart. Phys., 1210, 003
Marsh D. J. E., Ferreira P. G., 2010, Phys. Rev. D, 82, 103528
Marsh D. J. E., Pop A.-R., 2015, MNRAS, 451, 2479
Martinez-Medina L. A., Matos T., 2014, MNRAS, 444, 185
Martinez-Medina L. A., Robles V. H., Matos T., 2015, Phys. Rev. D, 91, 023519
Matos T., Guzmán F. S., 1998, Class. Quantum Gravity, 17, L9
Matos T., Arturo Ureña-López L., 2001, Phys. Rev. D, 63, 063506
Matos T., Guzman F. S., 2000, Class. Quantum Gravity, 17, L9
Matos T., Ureña-López L. A., 2000, Class. Quantum Gravity, 17, L75
Matos T., Guzman F., Urena-Lopez L. A., 2000, Class. Quantum Gravity, 17, 1707
Matos T., Avilez A., Bernal T., Chavanis P.-H., 2016, preprint (arXiv:1608.03945)
McConnell N. J., Ma C.-P., 2013, ApJ, 764, 184
McConnell N. J., Ma C.-P., Gebhardt K., Wright S. A., Murphy J. D., Lauer T. R., Graham J. R., Richstone D. O., 2011, Nature, 480, 215
McGaugh S. S., de Blok W. J. G., Schombert J. M., Kuzio de Naray R., Kim J. H., 2007, ApJ, 659, 149
McGaugh S. S., Lelli F., Schombert J. M., 2016, Phys. Rev. Lett., 117, 201101
Membrado M., Pacheco A. F., Sañudo J., 1989, Phys. Rev. A, 39, 4207
Menou K., Haiman Z., Narayanan V. K., 2001, ApJ, 558, 535
Merritt D., Ferrarese L., 2001, ApJ, 547, 140
Mocz P., Vogelsberger M., Robles V. H., Zavala J., Boylan-Kolchin M., Fialkov A., Hernquist L., 2017, MNRAS, 471, 4559
Moore B., Quinn T., Governato F., Stadel J., Lake G., 1999, MNRAS, 310, 1147
Myung Y. S., Kim Y.-W., Park Y.-J., 2008, Eur. Phys. J. C, 58, 617
Netzer H., 2003, ApJ, 583, L5
Ohashi A., Sakagami M.-a., 2004, Class. Quantum Gravity, 21, 3973
Pawlowski M. S., Pflamm-Altenburg J., Kroupa P., 2012, MNRAS, 423, 1109
Peebles P. J. E., 2000, ApJ, 534, L127
Peñarrubia J., Pontzen A., Walker M. G., Koposov S. E., 2012, ApJ, 759, L42
Plummer H. C., 1911, MNRAS, 71, 460
Press W. H., Ryden B. S., Spergel D. N., 1990, Phys. Rev. Lett., 64, 1084
Ricarte A., Dexter J., 2015, MNRAS, 446, 1973
Robles V. H., Matos T., 2012, MNRAS, 422, 282
Robles V. H., Matos T., 2013a, Phys. Rev. D, 88, 083008
Robles V. H., Matos T., 2013b, ApJ, 763, 19
Robles V. H., Martinez-Medina L. A., Matos T., 2015, preprint (arXiv:1503.00799)
Rodríguez-Montoya I., Magaña J., Matos T., Pérez-Lorenzana A., 2010, ApJ, 721, 1509
Ruffini R., Bonazzola S., 1969, Phys. Rev., 187, 1767
Sahni V., Wang L., 2000, Phys. Rev., 62, 103517
Sanchis-Gual N., Degollado J. C., Font J. A., Herdeiro C., Radu E., 2017, Class. Quantum Gravity, 34, 165001
Sarkar A., Mondal R., Das S., Sethi S. K., Bharadwaj S., Marsh D. J., 2016, J. Cosmol. Astropart. Phys., 2016, 012
Sawala T. et al., 2016, MNRAS, 457, 1931
Schive H.-Y., Chiueh T., Broadhurst T., 2014, Nat. Phys., 10, 496
Schive H.-Y., Chiueh T., Broadhurst T., Huang K.-W., 2016, ApJ, 818, 89
Schwabe B., Niemeyer J. C., Engels J. F., 2016, Phys. Rev. D, 94, 043513
Seidel E., Suen W.-M., 1990, Phys. Rev. D, 42, 384
Seidel E., Suen W.-M., 1991, Phys. Rev. Lett., 66, 1659
Seidel E., Suen W.-M., 1994, Phys. Rev. Lett., 72, 2516
Silk J., Rees M. J., 1998, A&A, 331, L1
Sin S.-J., 1994, Phys. Rev. D, 50, 3650
Strigari L. E., Bullock J. S., Kaplinghat M., Simon J. D., Geha M., Willman B., Walker M. G., 2008, Nature, 454, 1096
Suárez A., Chavanis P.-H., 2015, Phys. Rev. D, 92, 023510
Suárez A., Matos T., 2011, MNRAS, 416, 87
Ureña-López L. A., 2009, J. Cosmol. Astropart. Phys., 1, 014
Ureña-López L. A., Bernal A., 2010, Phys. Rev. D, 82, 123535
Ureña-López L. A., Gonzalez-Morales A. X., 2016, J. Cosmol. Astropart. Phys., 7, 048
Ureña-López L. A., Liddle A. R., 2002, Phys. Rev. D, 66, 083005
Ureña-López L. A., Robles V. H., Matos T., 2017, Phys. Rev. D, 96, 043005
Walker M., 2013, Dark Matter in the Galactic Dwarf Spheroidal Satellites. Springer Science+Business Media, Dordrecht, p. 1039, doi:10.1007/978-94-007-5612-0_20
Walker M. G., Mateo M., Olszewski E. W., Peñarrubia J., Wyn Evans N., Gilmore G., 2009, ApJ, 704, 1274
Wetterich C., 2001, Phys. Lett. B, 522, 5
Woo T.-P., Chiueh T., 2009, ApJ, 697, 850
Yu Q., Tremaine S., 2002, MNRAS, 335, 965

APPENDIX: SELF-GRAVITY IN THE NEWTONIAN LIMIT OF THE KLEIN–GORDON–POISSON SYSTEM

The fully relativistic regime of the system formed by a BH and a DM halo, ends up at small radii away from the centre. To give an idea of that, let us think in the Milky Way, where $2M \sim 10^{-4}$ pc. Therefore, at few parsecs away from the centre, the Newtonian limit is valid, that is for $r \gg 2M$ and the gravitational potential produced by the DM halo being $\Phi_{\rm h} \ll 1$. The metric describing the space–time at such region is approximately:

$$ds^2 = -\left(1 - \frac{2M}{r} + \Phi\right) dt^2 + \left(1 + \frac{2M}{r} - \Phi\right) dr^2 + r^2 d\Omega^2,$$

and the gravitational potential of the halo obeys the Poisson equation given by

$$\nabla^2 \Phi_{\rm h} = 4\pi G \phi^2, \tag{A1}$$

which in spherical symmetry can be approximated by

$$\frac{1}{r^2}\partial_r(r^2\partial_r\Phi_{\rm h}) = 4\pi G\phi^2,$$
$$\sim \frac{3}{r^2}\Phi_{\rm h} \sim 4\pi G\phi^2. \quad \text{(A2)}$$

On the other hand, the Klein–Gordon equation for the radial part of the scalar solution in this metric in the limit $r \gg 2M$ and $\Phi_{\rm h} \ll 1$ reads

$$k^2R + \frac{1}{r^2}\partial_r[r^2\partial_r R] + m^2\left(\frac{2M}{r} - \Phi_{\rm h}\right)R = 0. \quad \text{(A3)}$$

After plugging (A2) in the last equation, we have

$$k^2R + \frac{1}{r^2}\partial_r[r^2\partial_r R] + m^2\left[\frac{2M}{r} - r^2\left(\frac{4\pi}{3}G\rho_{\rm s}R^2\right)\right]R = 0. \quad \text{(A4)}$$

Assuming that the observer is placed in a region nearby the BH influence radius r_0 (defined as $4\pi\rho_{\rm s}r_0^2R^2 = 2M/r_0$, $r_0 \sim 100$ pc for the Milky Way), if $2M \ll r \ll m^{-1}$, the last term in equation (A4) (which roughly accounts for self-gravity effects of the scalar halo nearby the centre) can be dropped away. In a region even further from the influence region, $R \sim \sin(kr)/r$, if $r < r_{\rm s}$ and then $R \sim k$ and equation (A4) becomes

$$k^2R + \frac{1}{r^2}\partial_r[r^2\partial_r R] + m^2\left[\frac{2M}{r} - (kr)^2\left(\frac{4\pi}{3}G\rho_{\rm s}\right)\right]R = 0. \quad \text{(A5)}$$

Under the considered conditions, we have demonstrated that if $2M \ll r \ll r_{\rm s}$, the last two terms in equation (A5) can be ignored.

This paper has been typeset from a TEX/LATEX file prepared by the author.